Censoring-Based Cooperative Spectrum Sensing with Improved Energy Detectors and Multiple Antennas in Fading Channels

SRINIVAS NALLAGONDA, Member, IEEE
Marri Laxman Reddy Institute of Technology and Management, Dundigal, India

SANJAY DHAR ROY, Member, IEEE
SUMIT KUNDU, Senior Member, IEEE
National Institute Technology, Durgapur, India

GIANLUIGI FERRARI, Senior Member, IEEE
RICCARDO RAHELI, Senior Member, IEEE
University of Parma, Parma, Italy

In this paper, the performance of cooperative spectrum sensing (CSS) with threshold-based censoring is investigated in the presence of noisy and faded environments. In particular, scenarios with Rayleigh, Hoyt, and Rician fading, affecting both the sensing (S) and reporting (R) channels, are considered. Each secondary user (SU) is equipped with multiple antennas and relies on an improved energy detector (IED). More precisely, the signals from the primary user (PU), received by multiple antennas of an SU, are fed to the IED, the IED outputs are combined using a selection combiner, and the combined signal is used to make a local decision. At the fusion center (FC), censoring of SUs is done on the basis of the quality, evaluated by the FC, of the faded R-channels. The censored decisions received at the FC are fused, using majority logic or maximal ratio combining, to obtain a final decision on the status of the PU. The performance of CSS, in terms of average miss detection probability and error rate, is evaluated considering the impact of relevant network parameters. Optimized values of the censoring threshold, as well as of the required parameters of the IED, are determined under several network conditions. The performance of the proposed IED is compared with that of a conventional energy detector.

Manuscript received May 6, 2016; revised October 21, 2016 and April 12, 2017; released for publication June 5, 2017. Date of publication July 27, 2017; date of current version April 11, 2018.

DOI. No. 10.1109/TAES.2017.2732798

Refereeing of this contribution was handled by D. Ciuonzo.

This work was presented in part at the IEEE INDICON Conference, IIT Bombay, India, December 2013, and at the IEEE ANTS Conference, India, December 2013.

Authors' addresses: S. Nallagonda is with the Department of Electronics and Communication Engineering, Marri Laxman Reddy Institute of Technology and Management, Dundigal 500043, India, E-mail: (srinivas.nallagonda@gmail.com); S. D. Roy and S. Kundu are with the Department of Electronics and Communication Engineering, National Institute Technology, Durgapur 713209, India, E-mail: (s_dharroy@yahoo.com; sumit.kundu@ece.nitdgp.ac.in); G. Ferrari and R. Raheli are with the Department of Engineering and Architecture, University of Parma, Parma 43124, Italy, E-mail: (gianluigi.ferrari@unipr.it; raheli@unipr.it). *(Corresponding author: Srinivas Nallagonda.)*

I. INTRODUCTION

Cognitive communications based on the use of spectrum sharing are a promising technology to make spectrum utilization efficient. In cognitive radio (CR) networks, secondary users (SUs) can access the licensed spectrum if the primary users (PUs) are sensed as idle on such spectrum. More precisely, the CR technology plays a significant role in making the best use of scarce spectrum to support the increasing demand for emerging wireless applications, e.g., TV bands for smart grid, military and public safety, broadband cellular, and the body area networks for medical applications [1], [2]. CR techniques could also be applied to satellite communication systems in several different ways. A secondary system can operate at the satellite bands using the cognitive principles to avoid interfering with the primary satellite system [3]. Spectrum sensing is an important feature of CR technology, since SUs need to detect the presence of PUs accurately and quickly, particularly when the PU signal information is unknown. In such scenarios, an appropriate choice is spectrum sensing using energy detection. An energy detector (ED) measures the energy in the received waveform over an observation time window [4]. The problem of designing the sensing duration to maximize the achievable throughput for the secondary network is studied in [5] and [6], under the constraint that the PUs are sufficiently protected. In [5] and [6], the sensing-throughput tradeoff problem is mathematically formulated and it is proven that the formulated problem has indeed one optimal sensing period which yields the highest throughput for the secondary network.

The performance of a single SU using a conventional energy detector (CED) is limited by severe fading or shadowing in the sensing channel (S-channel) between the PU and an SU [7]. By considering multiple cooperating SUs with CEDs, it is possible to improve the detection performance by having all SUs sense the PU individually and send their sensed information to a secondary fusion center (FC) through reporting channels (R-channels) [8]. The performance of cooperative spectrum sensing (CSS) can be improved further by utilizing an improved energy detector (IED) at each SU. In particular, the IED is obtained from the CED by replacing the squaring operation on the received signal amplitude with a power operation with properly optimized positive exponent [9]–[13]. In [14], an efficient decision fusion technique is studied for CSS with the logical OR-rule for dynamic spectrum sharing among PUs and SUs, respectively. A soft combination scheme is investigated in [15], where the accurately sensed energies from different CR users are combined to improve the decision correct-

ness. An optimal soft combination scheme that maximizes the detection probability for a given false alarm probability is also obtained by applying the Neyman–Pearson criterion. Maximal ratio combining (MRC) and equal gain combining (EGC) rules at the FC are employed and the performance is evaluated in terms of complementary receiver operating characteristic (CROC) curves [16].

The presence of fading in an R-channel, i.e., a channel connecting an SU with the FC is likely to affect the decisions sent by SUs (e.g., when the FC is far from the SU). If the aforementioned R-channel is deeply faded or shadowed, the decisions received at the FC from the corresponding SUs are likely to be erroneous. In this context, it is wise to stop transmitting decisions from these SUs: Censoring is thus expedient. The SUs, whose R-channels are estimated as reliable by the FC, are censored, i.e., they are allowed to transmit their decisions. If an SU is selected to transmit its local decisions to an FC, it does so using the R-channel with binary phase shift keying (BPSK) signaling. At the opposite, the SUs with unreliable (i.e., low quality) R-channels are prevented from transmitting, so that transmitting energy and transmission band of SUs can be saved. As the censoring scheme depends on the estimation of the fading levels of the R-channels by the FC, one can have two different censoring scenarios, depending on perfect or imperfect channel estimation, respectively. For example, minimum mean square error (MMSE)-based channel estimation can be used by the FC. In [17], censoring is applied to a decentralized detection problem. In this context, the optimal decision rules and the associated detection and false alarm probabilities have also been derived for different levels of channel state information availability for distributed detection in sensor networks over fading channels. In [18], sensors observe a physical phenomenon over faded S-channels and transmit their observations using the amplify-and-forward scheme over faded R-channels to the FC, which is equipped with multiple antennas. The sufficiency and optimality of ED for multi-input multioutput decision fusion in wireless sensor networks (WSNs) over nonline-of-sight fading scenarios are analyzed in [19].

A. Related Work

In [12] and [13], the performance of a CSS system with IEDs is only evaluated under the assumption that the S-channel is either a Hoyt-, Rayleigh-, or Rician-faded channel and the R-channel is ideal. However, in [12] and [13], censoring of IED-based SUs is not considered. In this work, we consider that both S- and R-channels are faded (Hoyt, Rayleigh, Rician). The transmission through deeply faded R-channels can be stopped by threshold-based censoring. The performance of CSS with threshold-based censoring of CEDs in the presence of Rayleigh [20] and Hoyt [21] fading is investigated. In [22], rank-based censoring of IED is evaluated in the presence of Rayleigh fading, considering OR-logic, AND-logic, and majority-logic fusion rules at FC. It is shown that the total error probability (given by the sum of miss detection and false alarm probabilities) is the same for both AND-logic and OR-logic fusion rules and is higher than the error probability with majority-logic fusion for a large number of CR users. In [23], censoring of SUs on the basis of the received energy is discussed. In particular, an SU does not send any decision if the energy value lies between two thresholds. However, in this work, censoring of SUs based on the R-channel quality is considered. This has motivated us to develop suitable analytical and simulation frameworks for IED-based CSS systems with threshold-based censoring in Rayleigh-, Hoyt-, and Rician fading channels for an energy-constrained CR network. It is known that, depending on the particular propagation environment and the underlying communication scenario, several fading models have been devised. The Rayleigh distribution is used to model the propagation environment, where the mobile antenna receives a large number of reflected and scattered waves. The Nakagami-n distribution, known as the Rician distribution, is often used to model environments characterized by Rayleigh fading channels, except that the set of reflected and scattered waves is dominated by one strong component [24]. The Hoyt distribution, also known as Nakagami-q distribution (q being the fading severity parameter), allows us to span the range of fading distribution from one-sided Gaussian ($q = 0$) to Rayleigh ($q = 1$), and is used extensively to model more severe than Rayleigh fading wireless links. The Hoyt distribution is typically applied to satellite links affected by strong ionospheric scintillation [24]–[26]. In [27], an overview of the classic problem of testing samples drawn from independent homogeneous Bernoulli probability mass functions (pmfs) is investigated, in scenarios where the success probabilities under the alternative hypothesis are not known. A closed-form expression for the pmf for discrete random variables is derived in [28]: it describes the numbers of successes in a sequence of independent trials, when the individual probabilities of success vary across trials. Several of its advantages, in terms of computational speed, implementation, and simplification of analysis are also discussed. In [29]–[31], the channel-aware decision fusion rules are developed for a WSN, where binary decisions from local sensors are relayed through multihop transmission in order to reach an FC.

B. Overview of This Paper

This paper investigates the joint impact of threshold-based censoring and multiple antenna-based IED on the overall detection performance of a spectrum sensing scheme, using two fusion rules, namely majority logic and MRC. In connection with censoring based on reporting channel, the impact of channel estimation errors on overall performance is also investigated. Several fading models, namely, Rayleigh, Rician, Hoyt, are considered in the R-channel. The average miss detection probability and error rate are selected as the key performance metrics. Although miss detection and false alarm probabilities are conventionally used to characterize the performance of CSS schemes (and, generally, one can be traded off for the other), the error rate concisely characterizes the overall system performance

TABLE I
Performance Metric Under Case Study

Case study	Performance metrics
Single SU	$(P_m + P_f)$: error rate at SU
	P_m: miss detection probability at SU
	P_f: false alarm probability at SU
CSS without censoring	$(Q_m + Q_f)$: error rate at FC
	Q_m: miss detection probability at FC
	Q_f: false alarm probability at FC
CSS with censoring	$(\bar{Q}_m + \bar{Q}_f)$: error rate at FC
	$\bar{Q}_m$: average miss detection probability at FC
	$\bar{Q}_f$: average false alarm probability at FC

[9]–[13]. Hence, minimization of the error rate will lead to selecting an optimized operating point, where none of the conventional error metrics (i.e., miss detection and false alarm probabilities) is penalized too much with respect to the other. We have considered several performance metrics depending on the cases under study. More precisely, the following three cases are considered:

1) performance analysis of IED-based single SU;
2) performance analysis of IED-based multiple SUs;
3) performance analysis of IED-based multiple SUs with censoring.

For each of the three scenarios, various fading conditions are investigated. The case studies and their corresponding metrics have been summarized in Table I.

The main contributions of this work can be summarized as follows.

1) We derive an analytical expression of the error rate for a CSS system without censoring (ideal or noiseless R-channels), using a counting (or k-out-of-N fusion) rule at the FC, in additive white Gaussian noise (AWGN), Rayleigh-, Hoyt-, and Rician-faded sensing environments. The performance results, in terms of error rate, are novel and have not appeared in the literature, yet.
2) We investigate the performance of CSS systems with threshold-based censoring of multiple IEDs, and compare it with the performance of CEDs. It is shown that an IED-based sensing system with threshold-based censoring shows a significant performance improvement with respect to conventional sensing systems (i.e., CED-based) [20], [21].
3) We derive an expression for the probability of selecting an SU in the presence of a Rician-faded channel. This expression is very useful to find the probability of selecting some of SUs, out of the entire set of SUs, for CSS systems with threshold-based censoring. We develop a suitable analytical framework and carry out simulations for performance evaluation under both perfect and imperfect MMSE-based estimation of R-channel.
4) We derive an expression for error variance when the R-channel is either Hoyt or Rician faded. We then find channel error coefficients when the R-channel is imperfect. On the basis of available perfect and imperfect channel coefficients, suitable analytical and simulation frameworks are developed for the proposed IED-based CSS systems with threshold-based censoring.
5) We investigate the joint impact of threshold-based censoring and diversity-based IED on the overall detection performance using majority-logic and MRC fusion rules. The impacts of several network parameters (including the IED parameter, the number of antennas, the normalized detection threshold, the censoring threshold, the available number of SUs in the network, the average S-channel and R-channel signal-to-noise ratios, SNRs) on the performance of CSS systems are investigated. Optimized values of the censoring threshold are determined, in several network conditions, in order to minimize the miss detection probability and the error rate. The optimal values of a) the normalized detection threshold λ_n, b) the IED parameter p, and c) the number N of SUs are determined as functions of several network parameters. In [12] and [13], these values were not identified.

The formulation presented here could be extended to the frequency-selective fading channel, however such an extension is beyond the scope of this paper and will not be further discussed. This work on distributed detection with CR is useful in designing electronic systems to detect any phenomena from the observations of cognitive sensor nodes subjected to various fading conditions in the channel. Furthermore, the concept of our work could be useful in the context of aeronautical communication systems such as air to air, air to ground communication systems, wireless avionics systems, where aeronautical spectrum is congested due to growing demand and at the same time underutilized due to static allocation [32].

The rest of the paper is organized as follows. In Section II, the system model is described. Analytical and simulation results of IED-based CSS systems without censoring are presented and discussed in Section III. In Section IV, the proposed analytical framework is extended to incorporate censoring scenarios, where the R-channel is noisy and faded. In Section V, the performance of CSS with censoring is investigated. Finally, Section VI concludes the paper.

II. SYSTEM MODEL

The proposed system model is shown in Fig. 1. It consists of N SUs, one secondary FC, and one PU. We assume that the PU and the FC are equipped with transmit/receive single antenna, whereas each SU is equipped with M receive antennas, IED, and a single transmit antenna. All SUs forward their sensing information to the FC through the R-channel. More precisely, each SU receives the signals from its M antennas and processes them with corresponding IEDs. The energy values available at the output of the IEDs (just before taking hard decisions) are combined using SC. The highest energy value is selected and is first compared with a local detection threshold, denoted as λ (all SUs are assumed to have the same value of λ); then, a hard local decision about the status (presence or absence)

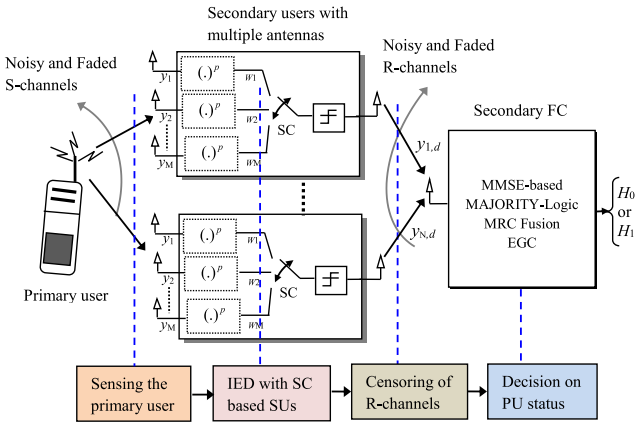

Fig. 1. Considered system model: CSS with censoring.

of the PU is made. The R-channels are either ideal (without censoring) or noisy-faded (with censoring). The PU is assumed to be closer to the SUs, so that the S-channel SNR is increased. We remark, however, that our model is general and can be used for any SNRs' configuration. In the presence of censoring, both S- and R-channels are noisy and faded, namely 1) noisy-Rayleigh faded, 2) noisy-Hoyt faded, and 3) noisy-Rician faded.

The received signal at the ith antenna ($i = 1, 2, \ldots, M$) at each SU can be expressed as

$$y_i(n) = \begin{cases} n_i(n) & \mathcal{H}_0 \\ h_i s(n) + n_i(n) & \mathcal{H}_1 \end{cases} \tag{1}$$

where $s(n)$ is assumed as an unknown signal from the PU with energy E_s as in [9]; $\{n_i(n)\}_{i=1}^{M}$ are independent and identically distributed zero-mean circularly symmetric complex Gaussian random variables, i.e., $n_i(n) \sim \mathcal{CN}(0, \sigma_n^2)$, where σ_n^2 is the noise variance; h_i is the S-channel fading coefficient at the ith antenna at each SU, also modeled as circularly symmetric complex Gaussian, with both mean and variance depending on the type of fading; and $\mathcal{H}_1$ and $\mathcal{H}_0$ are the two hypotheses associated with the presence and the absence of a PU, respectively. We assume that $\{h_i\}$ are independent. The decision variable, denoted as W_i, at the ith antenna at each SU for deciding on the presence or absence of the PU is [9]–[12]

$$W_i = |y_i|^p \tag{2}$$

where $p > 0$ is the IED parameter. From (2), it can be concluded that W_i reduces to the decision variable of a CED for $p = 2$ [7]. The general expressions for the false alarm and miss detection probabilities are given in [35, eq. (41), chapter 2] as

$$P_f = \int_{\lambda}^{\infty} f_{Z|\mathcal{H}_0}(z)dz = 1 - F_{Z|\mathcal{H}_0}(\lambda); \quad Z \geq 0, \tag{3}$$

$$P_m = \int_{0}^{\lambda} f_{Z|\mathcal{H}_1}(z)dz = F_{Z|\mathcal{H}_1}(\lambda); \quad Z \geq 0 \tag{4}$$

where $f_{Z|\mathcal{H}_0}(z)$ and $f_{Z|\mathcal{H}_1}(z)$ are the conditional probability density functions (PDFs) of the decision variable Z, under hypotheses $\mathcal{H}_0$ and $\mathcal{H}_1$, respectively. The cumulative distribution function (CDF) of the IED at each antenna can be written as [9]–[12]

$$F_{W_i|\mathcal{H}_j}(x) = \Pr\left[|y_i|^p|_{\mathcal{H}_j} \leq x\right]_{j=0,1} \tag{5}$$

where $\Pr[\cdot]$ denotes probability. Each SU evaluates its decision variables (i.e., $\{W_i\}_{i=1}^{M}$) for all M antennas and uses the SC diversity technique that outputs the maximum value out of M decision variables evaluated for different diversity branches, i.e., $Z = \max\{W_1, W_2, \ldots, W_M\}$. The conditional CDF with SC, under hypothesis $\mathcal{H}_0$, is given by [9]–[12]

$$F_{Z|\mathcal{H}_0}(z) = \left[1 - \exp\left(-\frac{z^{2/p}}{\sigma_n^2}\right)\right]^M. \tag{6}$$

The output of the SC is now applied to a binary hard detector which takes a decision in the presence or absence of a PU as follows [9]–[12]:

$$Z \underset{0}{\overset{1}{\gtrless}} \lambda \tag{7}$$

where the detection threshold λ at an SU can be expressed as $\lambda = \lambda_n \sigma_n^p$, with λ_n being the normalized detection threshold (to be determined) and σ_n the noise standard deviation. All SUs are assumed to have the same IED (power p operation) with the same detection threshold. The λ_n is set by normalizing λ with a factor involving p following [9]. From (3), (6), and (7), the false alarm probability P_f at an SU can be expressed as [12]

$$P_f = 1 - \left[1 - \exp\left(-\frac{\lambda^{2/p}}{\sigma_n^2}\right)\right]^M. \tag{8}$$

We remark that P_f is the same for any fading environment since, under $\mathcal{H}_0$, there is no PU signal. Therefore, it will not be further discussed.

A. Nonfaded (AWGN) Environment

In a nonfaded (AWGN) environment, the channel gains can be considered as fixed and, thus, normalized to $h_i = 1, \forall i \in \{1, \ldots M\}$. Using [36, eq. (9)], the expression for the miss detection probability in AWGN channels can be obtained [12]:

$$P_m^{\text{AW}} = \left[1 - Q\left(\sqrt{\frac{2E_s}{\sigma_n^2}}, \lambda^{1/p}\sqrt{\frac{2}{\sigma_n^2}}\right)\right]^M \tag{9}$$

where $Q(a, b) \triangleq \int_b^{\infty} x \exp\left(-\frac{x^2+a^2}{2}\right) I_0(ax)\mathrm{d}x$ is the first-order Marcum Q-function [33].

B. Rayleigh-Faded Environment

In a Rayleigh-faded environment, each channel gain h_i is a circularly symmetric zero mean complex Gaussian random variable with variance σ_h^2, i.e., $h_i \sim \mathcal{CN}(0, \sigma_h^2)$. The miss detection probability can be expressed as [12]

$$P_m^{\text{Ra}} = \left[1 - \exp\left(-\frac{\lambda^{2/p}}{\sigma_n^2(1 + \bar{\gamma}_s)}\right)\right]^M \tag{10}$$

where $\bar{\gamma}_s = E_s\sigma_h^2/\sigma_n^2$ is the average SNR of the link between a PU and an SU.

Using (9) and (10), the optimal detection threshold (denoted as λ_{opt}), i.e., the threshold in correspondence to which the total error rate ($P_m^{\text{Ra}} + P_f$) of a single SU is minimized, can be obtained. In order to find λ_{opt}, a first-order partial derivative of $P_m^{\text{Ra}} + P_f$ with respect to λ is performed for fixed values of p and $\bar{\gamma}_s$ and the result is set to zero, i.e., $\partial(P_m^{\text{Ra}} + P_f)/\partial\lambda = 0$. It may be noted that it is difficult to track analytically λ_{opt} for a general case of M antennas. However, the following closed-form expressions of λ_{opt} for $M = 1$ and $M = 3$ can be obtained: $[\sigma_n^2(1+\bar{\gamma}_s)\ln(1+\bar{\gamma}_s)/\bar{\gamma}_s]^{p/2}$ and $[\sigma_n^2(1+\bar{\gamma}_s)\ln(1+\bar{\gamma}_s)/2\bar{\gamma}_s]^{p/2}$.

C. Hoyt or Nakagami-q Fading Environment

For a Hoyt- or Nakagami-q-faded environment, the fading coefficient at the ith antenna h_i ($i = 1, \ldots, M$) can be modeled as a complex Hoyt random variable [25, Eq. (45)]. The conditional PDF of W_i, under hypothesis $\mathcal{H}_1$, can be derived using a proper random variable transformation as

$$f_{W_i|\mathcal{H}_1}^{\text{Ho}}(y) = \frac{y^{\frac{2}{p}-1}}{p\sigma_1\sigma_2}\exp\left[-\frac{y^{\frac{2}{p}}}{4}\left(\frac{1}{\sigma_1^2}+\frac{1}{\sigma_2^2}\right)\right] \times I_0\left[\frac{y^{\frac{2}{p}}}{4}\left(\frac{1}{\sigma_2^2}-\frac{1}{\sigma_1^2}\right)\right]; \quad i = 1, \ldots, M \tag{11}$$

where $\sigma_1^2 = E_s\sigma_{h1}^2 + \sigma_n^2/2$; $\sigma_{h1} = \sqrt{\Omega q^2/1+q^2}$; $\sigma_2^2 = E_s\sigma_{h2}^2 + \sigma_n^2/2$; $\sigma_{h2} = \sqrt{\Omega/1+q^2}$; Ω is the average fading power, normalized to unity; $I_0(.)$ is the first-order modified Bessel function; and $q \in (0, 1)$ is the Hoyt fading parameter. After a few algebraic manipulations using [26, Eq. (58)], the conditional CDF with SC under $\mathcal{H}_1$ can be expressed as follows:

$$F_{Z|\mathcal{H}_1}^{\text{Ho}}(z) = \frac{1}{16}\left[1 + \exp(-\mathcal{A}z^{2/p})I_0(\mathcal{B}z^{2/p}) - 2Q(\mathcal{U}_1, \mathcal{V}_1)\right]^M \tag{12}$$

where $\mathcal{A} = (1/\sigma_2^2 + 1/\sigma_1^2)/4$; $\mathcal{B} = (1/\sigma_2^2 - 1/\sigma_1^2)/4$; $\mathcal{U}_1 = \sqrt{(\mathcal{A}-\sqrt{\mathcal{A}^2-\mathcal{B}^2})z^{2/p}}$; and $\mathcal{V}_1 = \sqrt{(\mathcal{A}+\sqrt{\mathcal{A}^2-\mathcal{B}^2})z^{2/p}}$.

The miss detection probability can be obtained from (4), (7), and (12) as

$$P_m^{\text{Ho}} = \frac{1}{16}\left[1 + \exp(-\mathcal{A}\lambda^{2/p})I_0(\mathcal{B}\lambda^{2/p}) - 2Q(\mathcal{U}_2, \mathcal{V}_2)\right]^M \tag{13}$$

where $\mathcal{U}_2 = \sqrt{(\mathcal{A}-\sqrt{\mathcal{A}^2-\mathcal{B}^2})\lambda^{2/p}}$ and $\mathcal{V}_2 = \sqrt{(\mathcal{A}+\sqrt{\mathcal{A}^2-\mathcal{B}^2})\lambda^{2/p}}$.

D. Rician or Nakagami-n Fading Environment

In the presence of Rician or Nakagami-n fading h_i at the ith receive antenna, the PDF of $|h_i|$ ($i \in \{1, \ldots, M\}$) is characterized by a Rician distribution [24] and the complex fading coefficient has the normal distribution $\mathcal{CN}(s, \sigma_h^2)$, where the average value s can be assumed to be real. The real Rician fading parameter $K > 0$ is the ratio between the direct path signal power and the scattered signal component power, i.e.,

$$K = s^2/\sigma_h^2. \tag{14}$$

The total fading power is $\mathbb{E}\{|h_i|^2\} = s^2 + \sigma_h^2$ and accounts for both direct and scattered components. Assuming that the fading power is normalized, i.e., $\mathbb{E}\{|h_i|^2\} = \Omega = 1, \forall i \in \{1, \ldots M\}$, one obtains

$$\sigma_h = 1/\sqrt{1+K} \quad s = \sqrt{K/(1+K)}. \tag{15}$$

Conditionally on hypothesis $\mathcal{H}_1$, the received signal has distribution: $y_i \sim \mathcal{CN}(s\sqrt{E_s}, E_s\sigma_h^2 + \sigma_n^2)$. Since $|y_i|$ has a Rician distribution, the conditional PDF of $W_i = |y_i|^p$, under hypothesis $\mathcal{H}_1$, can be obtained through a random variable transformation, obtaining

$$f_{W_i|\mathcal{H}_1}^{\text{Ri}}(y) = \frac{2y^{(2/p)-1}}{p(E_s\sigma_h^2+\sigma_n^2)}\exp\left(-\frac{y^{2/p}+s^2E_s}{E_s\sigma_h^2+\sigma_n^2}\right) \times I_0\left(\frac{2s\sqrt{E_s}y^{1/p}}{E_s\sigma_h^2+\sigma_n^2}\right). \tag{16}$$

The conditional CDF with SC under hypothesis $\mathcal{H}_1$ is

$$F_{Z|\mathcal{H}_1}^{\text{Ri}}(z) = \left[1 - Q\left(\sqrt{\frac{2E_s}{E_s\sigma_h^2+\sigma_n^2}}, z^{1/p}\sqrt{\frac{2}{E_s\sigma_h^2+\sigma_n^2}}\right)\right]^M. \tag{17}$$

Finally, from (4), (7), and (17), the miss detection probability can be expressed as

$$P_m^{\text{Ri}} = \left[1 - Q\left(\sqrt{\frac{2E_s}{\sigma_n^2(1+\bar{\gamma}_s)}}, \lambda^{1/p}\sqrt{\frac{2}{\sigma_n^2(1+\bar{\gamma}_s)}}\right)\right]^M. \tag{18}$$

III. PERFORMANCE ANALYSIS OF CSS: IDEAL REPORTING CHANNELS

The detection performance can be improved by allowing different SUs (N) to cooperate by sharing their information. Each SU makes its own local decision regarding the presence or absence of a PU (i.e., $\mathcal{H}_1$ or $\mathcal{H}_0$), and forwards the binary decision ("1" or "0") to the FC for data fusion. We assume that SUs have identical local performances. The generalized counting rules (also denoted as k-out-of-N fusion rule) for the probabilities of miss detection (Q_m) and false alarm (Q_f) at the FC are given by [8], [27], [28]

$$Q_m = 1 - \sum_{\ell=k}^{N}\binom{N}{\ell}(1-P_m)^{\ell}(P_m)^{N-\ell}, \tag{19}$$

$$Q_f = \sum_{\ell=k}^{N}\binom{N}{\ell}(P_f)^{\ell}(1-P_f)^{N-\ell} \tag{20}$$

where P_m and P_f are the probabilities of miss detection and false alarm at each individual SU, as derived in Section II. Expressions for probabilities Q_m and Q_f under OR-logic, AND-logic, and majority-logic fusion rules can be derived by setting $k = 1$, $k = N$, and $k = \lfloor N/2 \rfloor$ in (19) and (20), respectively, where $\lfloor . \rfloor$ indicates the largest integer not greater than the argument. Therefore, the error rate

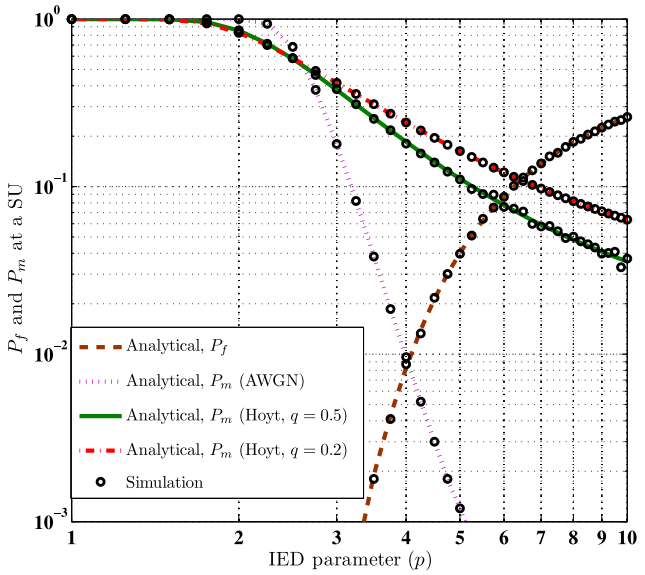

Fig. 2. Performance of a single SU (P_m and P_f as function of p) in AWGN channel and Hoyt fading channel ($q = 0.2$, and 0.5), with $\bar{\gamma}_s$ =10 dB and $\lambda_n = 30$.

at the FC can be expressed as follows [34]:

$$Q = P(\mathcal{H}_1)Q_m + P(\mathcal{H}_0)Q_f. \tag{21}$$

In this paper, we assume that $P(\mathcal{H}_1) = P(\mathcal{H}_0) = 0.5$. However, we remark that the proposed approach is general. The system performance is investigated as a function of several system parameters, such as the number of SUs N, the number of receive antennas M at an SU, the IED parameter p, the average S-channel SNR $\bar{\gamma}_s$, and the normalized detection threshold λ_n. The counting (or k-out-of-N fusion) rule is performed at the FC. The impact of fading on the system performance is also discussed. The performance is evaluated in terms of miss detection probability, false alarm probability, and error rate.

In Fig. 2, the performance of a single SU with $M = 2$ antennas and IED is shown. The probabilities of miss detection (P_m) and false alarm (P_f) are evaluated, as functions of p, with AWGN channels as well as with Hoyt fading channels. It can be observed that as p increases, with the other parameters kept fixed, P_m decreases and P_f increases. Our results show that P_m is highest and P_f is lowest for $p = 2$ (CED) with both AWGN and Hoyt channels. As p increases from 2 to 10, P_m decreases rapidly: more precisely, for $p = 4$, both P_m and P_f reach very low values (nearly zero) with AWGN channels. This is a great advantage of IED with respect to CED. The effect of the Hoyt fading on the miss detection probability is also investigated considering $q = 0.2$ and $q = 0.5$. It can be observed that P_m is a decreasing function of the fading parameter q. In the same figure, simulation results are also shown to validate our analytical framework presented in Section II. The value of p in correspondence to which both P_m and P_f reach sufficiently low values is identified as the optimum value of p. More precisely, assigning proper weights to P_m and P_f, a cost function can be defined and the value of p, which minimizes this cost can be found. In the special case of uniform weights equal to 0.5, this cost function is equal to the average error probability. From Fig. 2, one can conclude that the optimum values of p which minimize the average error probability are, respectively, 4 for the AWGN case and 5.8 for the Hoyt case with $q = 0.5$. Table II shows a direct comparison between the performance with CED ($p = 2$) and IED ($p = 4$), through receiver operating characteristic (ROC) curves, for various values of $\bar{\gamma}_s$ in Hoyt fading channel. The parameters M, λ_n, and q are set to 2, 10, and 1.0, respectively. It can be observed that spectrum sensing with IED outperforms spectrum sensing with CED for the same values of $\bar{\gamma}_s$ and P_f.

TABLE II
Comparison of CED and IED Through ROC (P_d, P_f)

$\bar{\gamma}_s$ (dB)	P_d for CED ($p = 2$) $P_f = 0.9 \times 10^{-4}$	P_d for IED ($p = 4$) $P_f = 0.9 \times 10^{-4}$
−10	2.25×10^{-4}	0.1097
−5	1×10^{-3}	0.1728
0	0.0134	0.3692
5	0.1728	0.7167
10	0.6435	0.9376

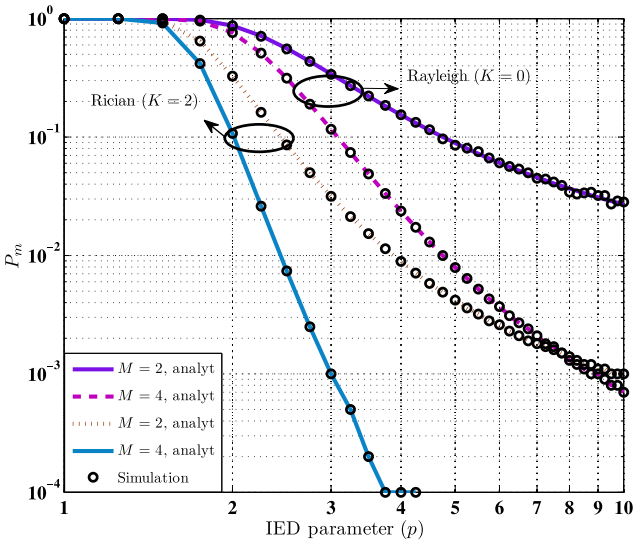

Fig. 3. Performance of a single SU (P_m versus p) in Rayleigh and Rician ($K = 0$ and 2) fading channels for various values of M ($\bar{\gamma}_s$ = 10 dB, $\lambda_n = 30$).

In Fig. 3, the performance of a single SU with multiple antenna-based IED in Rayleigh and Rician (K is set to either 0 or 2) fading channels is shown. As in Fig. 2, it can be observed that P_m is a decreasing function of p for both fading environments. It is found that for $p = 2$ (CED), $M = 2$, and Rayleigh fading, the optimal value of p_m is 0.9, whereas it is 0.17 for $p = 4$ (IED) for the same value of M. It can be observed that an SU with IED (for $p > 2$) leads to an improved performance with respect to an SU with CED (for $p = 2$) for a fixed values of λ_n and number of antennas. The performance improves further for increasing values of M. The performance with Rician fading parameter set to 0 corresponds to the case with Rayleigh fading. A

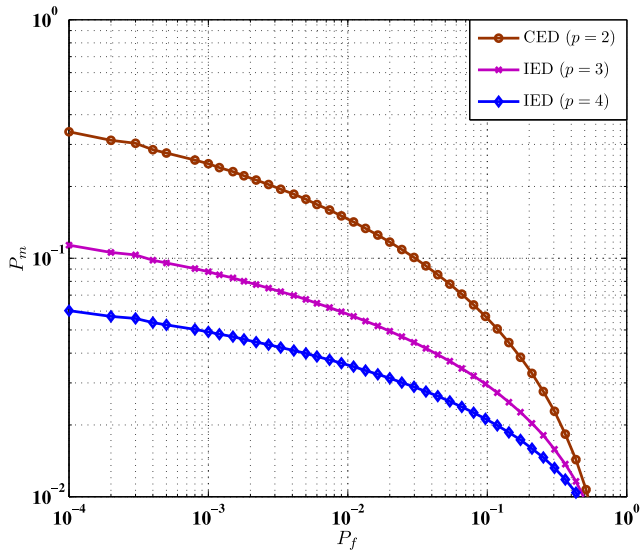

Fig. 4. Performance comparison between CED and IED through CROC (P_m versus P_f) curves in Rayleigh-faded channel ($\bar{\gamma}_s = 10$ dB, $M = 2$, $\lambda_n = 30$).

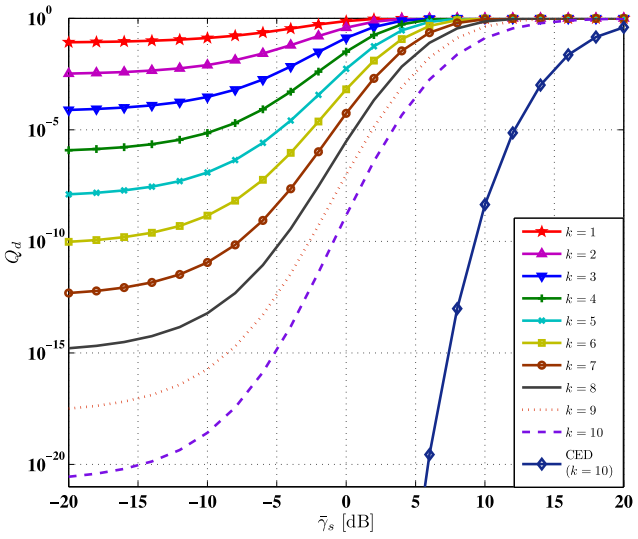

Fig. 5. Q_d versus $\bar{\gamma}_s$ for k-out of-N fusion rule, with Hoyt ($q = 0.5$) fading channel, $p = 4$, $M = 2$, $N = 10$, $\lambda_n = 30$, $Q_f = 0.08$.

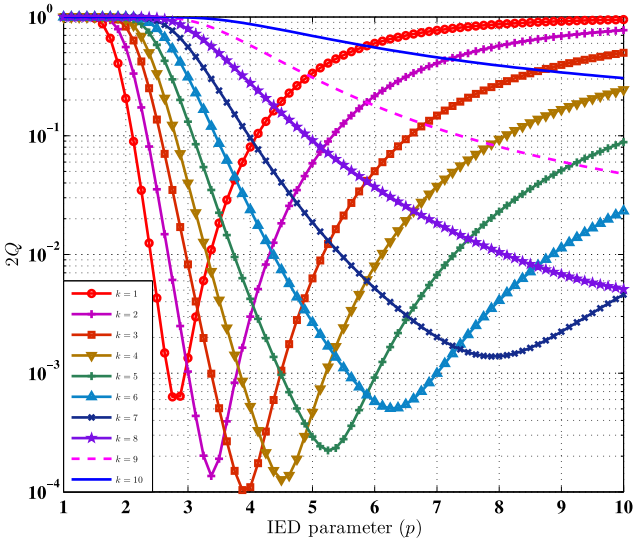

Fig. 6. $2Q$ versus p, for k-out-of-N fusion, with Hoyt ($q = 0.5$) fading channel, $\lambda_n = 30$, $M = 2$, $N = 10$, and $\bar{\gamma}_s = 10$ dB.

significant performance improvement is obtained when the Rician fading parameter increases to 2 (i.e., the severity of fading in the S-channel decreases). The simulation-based results match with the results based on the analytical expressions in both cases with Rayleigh- and Rician-faded environments.

Fig. 4 shows CROC comparisons between CED and IED for various values of parameter p. In the figure, $p = 2$ corresponds to CED and $p > 2$ corresponds to IED. It can be observed that for a fixed value of P_f, the performance of IED ($p > 2$) is better than that of CED ($p = 2$). For example, for $P_f = 1 \times 10^{-3}$, it is found that P_m is 0.2489 for CED, 0.0878 for IED with $p = 3$, and 0.0491 for IED with $p = 4$. It is found that P_m reduces by 80.27% when CED is replaced with IED ($p = 4$) for a fixed value of P_f equal to 1×10^{-3}.

In Fig. 5, the probability of detection (Q_d) is shown as a function of the average S-channel SNR ($\bar{\gamma}_s$) under Hoyt ($q = 0.5$) fading scenario for a k-out-of-N fusion rule at FC. It can be observed that there is an excellent detection performance improvement when either k or $\bar{\gamma}_s$ increases. For $Q_d = 0.9$, cooperative sensing with $k = 10$ requires $\bar{\gamma}_s = 18$ dB, spectrum sensing with $k = 6$ requires $\bar{\gamma}_s = 9$ dB, and spectrum sensing with $k = 1$ only needs $\bar{\gamma}_s = 2$ dB for individual SUs, i.e., an SNR gain of 16 dB is achieved when k changes from 10 to 1. For comparison purposes, the curve for cooperative sensing with CED with $k = 10$ is also shown. It can be observed that for $Q_d = 0.4$ and $k = 10$, CED ($p = 2$)-based CSS requires $\bar{\gamma}_s = 20$ dB, while IED ($p = 4$)-based CSS only needs $\bar{\gamma}_s = 12$ dB for individual SUs, i.e., an SNR gain of 8 dB is achieved when CEDs are replaced with IEDs in the CSS system.

In Fig. 6, the error rate is shown as a function of the IED parameter p under Hoyt ($q = 0.5$) fading for k-out-of-N fusion rule at the FC. The obtained results show that an optimal pair of values of p and N (in correspondence to which the error rate is minimized) can be found for all values of k (1 to 10 in the figure). The optimal pair of values of p and N is 4 and 4, respectively, i.e., $p = N = 4$.

In Fig. 7, the error rate is shown as a function of the normalized detection threshold λ_n, considering $p = 4$ and various values of the number N of SUs. Nonfaded (AWGN) and Hoyt-faded environments are considered. For Hoyt fading, two values of q (0.2 and 0.5) are considered. It can be observed that the error rate initially decreases, for increasing values of λ_n, and then increases, i.e., there is a minimum. A similar behavior is observed for all configurations of N and q. The optimum value of λ_n, for a given number of SUs and other fixed system parameters, is the value which minimizes the error rate. For example, in case of Hoyt ($q = 0.5$) fading channel, the optimum value of λ_n is 40 for $N = 3$, while it is 80 for $N = 6$. Similarly, for $N = 6$, the optimum value of λ_n is 75 and 80 for $q = 0.2$ and $q = 0.3$, respectively.

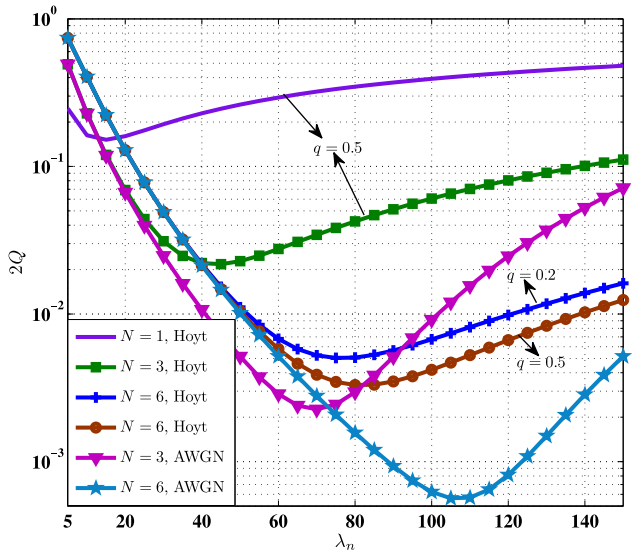

Fig. 7. $2Q$ versus λ_n, for various values of N, with AWGN channel and Hoyt ($q = 0.2$ and 0.5) fading channel, OR rule, $p = 4$, $M = 2$, and $\bar{\gamma}_s = 10$ dB.

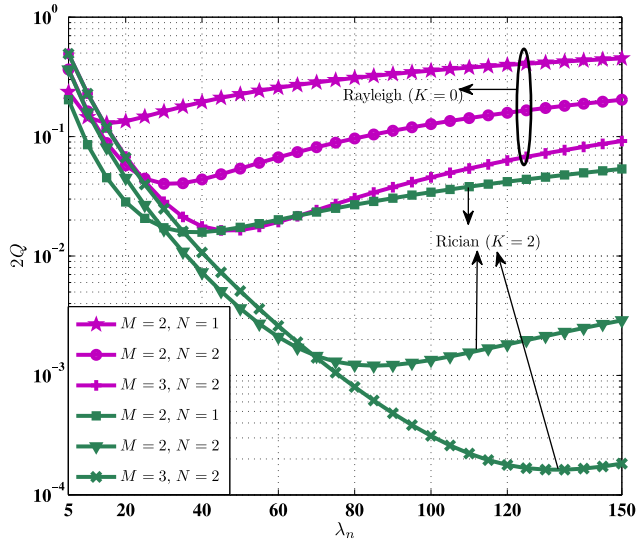

Fig. 8. $2Q$ versus λ_n for different values of M and N in Rayleigh and Rician ($K = 0$, and 2) fading channels, OR rule, $p = 4$, and $\bar{\gamma}_s = 10$ dB.

It is observed that as q increases from 0.2 to 0.3, the optimum value of λ_n increases and the error rate decreases significantly. As expected, in faded environments, the performance, in terms of error rate, degrades, with respect to the performance in a nonfaded environment, for any value of N.

In Fig. 8, the error rate is shown as a function of λ_n. The results are obtained by considering Rayleigh- and Rician-faded environments for various values of M and N. Several values of the Rician fading parameter ($K = 0, 2$), two values of M (2 and 4), and two different values of N (2 and 3) are considered. As in Fig. 7, it can be observed that the error rate initially decreases (for increasing values of λ_n) and then increases. A similar behavior can also be observed if N and M vary. For the Rician ($K = 2$) case, the optimum value of λ_n is 38 for $N = 1$ and $M = 2$ and 80 for $N = 2$ and $M = 2$. Similarly, for $K = 0$, $M = 2$, and $N = 2$, the optimum value of λ_n is 30, whereas it is 85 for $K = 2$ and the same values of M and N. As in Fig. 7, it can be observed that as the fading parameter K increases from 0 to 2, the optimum value of λ_n increases but the error rate decreases significantly. The error rate decreases further for increasing values of the number of antennas. For example, with Rician ($K = 2$) fading, when M increases from 2 to 3, the error rate decreases from 2×10^{-3} to 1×10^{-4}. From Figs. 7 and 8, it can also be observed that the error rate is very high for noncooperative ($N = 1$) spectrum sensing, with respect to cooperative spectrum sensing ($N > 1$), in any faded environment.

IV. CENSORING OF SUs BASED ON THE REPORTING CHANNEL QUALITY

At each SU, the decision variable Z is compared with its detection threshold λ to make a hard binary decision on the presence of a PU. If an SU is censored, i.e., it is allowed to transmit, its local decision is sent to the FC using BPSK over the corresponding faded R-channel.

A. Estimation of Fading Channel Coefficient in the R-Channel

Transmissions between the SUs and the FC are carried out in two phases. *In the first transmission phase,* the SUs send sequentially one training symbol each to enable the FC to estimate all N fading channel coefficients [38]. The MMSE estimation of the R-channel coefficients is considered at the FC using training symbols sent by the SUs to the FC. The signal from the kth SU received at the FC is

$$y_k = s_k h_k + n_k \qquad k \in \{1, 2, \ldots, N\} \tag{22}$$

where $s_k \in \{\sqrt{E_b}, -\sqrt{E_b}\}$ is a BPSK signal, whose two values correspond to $\mathcal{H}_1$ and $\mathcal{H}_0$, respectively. The R-channel coefficient h_k is modeled as a complex Gaussian random variable, whose mean and variance depend on the type of fading and $n_k \sim \mathcal{CN}\left(0, \sigma_n^2\right)$. The complex Gaussian channel noise samples $\{n_k\}$ and the fading R-channel coefficients $\{h_k\}$ are mutually independent. We assume that the FC estimates the kth SU's R-channel fading coefficient h_k according to an MMSE estimation strategy, on the basis of the observable y_k, as follows [20], [21], [38]:

$$\hat{h}_k = \mathbb{E}[h_k | y_k] = \frac{E_b}{E_b + \sigma_n^2} h_k + \frac{\sqrt{E_b}}{E_b + \sigma_n^2} n_k. \tag{23}$$

The estimation error for the kth R-channel, denoted as $\tilde{h}_k = h_k - \hat{h}_k$, can be expressed as

$$\tilde{h}_k = \frac{\sigma_n^2}{E_b + \sigma_n^2} h_k - \frac{\sqrt{E_b}}{E_b + \sigma_n^2} n_k. \tag{24}$$

From (24), since h_k and n_k are Gaussian, it can be concluded that the estimation error is also a complex Gaussian random variable. The mean and variance of $\tilde{h}_k$ depend on the type of fading, i.e., on the statistical distribution of the fading coefficient h_k.

1) *Rayleigh-Faded R-Channel:* For the kth Rayleigh-faded R-channel, the estimation error is $\tilde{h}_k \sim \mathcal{CN}(0, \sigma^2_{\tilde{h}_k})$. The variance $\sigma^2_{\tilde{h}_k}$ can be expressed as follows [38]:

$$\sigma^2_{\tilde{h}_k,\mathrm{Ra}} = \left(\frac{\sigma_n^2}{E_b+\sigma_n^2}\right)^2 + \frac{E_b\sigma_n^2}{(E_b+\sigma_n^2)^2} = \left(1+\frac{E_b}{\sigma_n^2}\right)^{-1} = \frac{1}{1+\bar{\gamma}_r} \tag{25}$$

where $\bar{\gamma}_r \triangleq E_b/\sigma_n^2$ is the average R-channel SNR.

2) *Hoyt-Faded R-Channel:* For the kth Hoyt-faded R-channel estimation error coefficient, the in-phase component $\tilde{h}_{kI}$ has the following distribution [21]:

$$\tilde{h}_{kI} \sim \mathcal{N}\left(0, \sigma^2_{\tilde{h}_{kI},\mathrm{Ho}}\right) \tag{26}$$

where

$$\sigma^2_{\tilde{h}_{kI},\mathrm{Ho}} = \left(\frac{\sigma_n^2}{E_b+\sigma_n^2}\right)^2 \frac{q^2}{1+q^2} + \frac{E_b\sigma_n^2}{2(E_b+\sigma_n^2)^2} = \left(1+\frac{1}{1+\bar{\gamma}_r}\right)^{-2}\left(\frac{q^2}{1+q^2}+\frac{1}{1+2\bar{\gamma}_r}\right). \tag{27}$$

Similarly

$$\tilde{h}_{kQ} \sim \mathcal{N}\left(0, \sigma^2_{\tilde{h}_{kQ},\mathrm{Ho}}\right) \tag{28}$$

where

$$\sigma^2_{\tilde{h}_{kQ},\mathrm{Ho}} = \left(\frac{\sigma_n^2}{E_b+\sigma_n^2}\right)^2 \frac{1}{1+q^2} + \frac{E_b\sigma_n^2}{2(E_b+\sigma_n^2)^2} = \left(1+\frac{1}{1+\bar{\gamma}_r}\right)^{-2}\left(\frac{1}{1+q^2}+\frac{1}{1+2\bar{\gamma}_r}\right). \tag{29}$$

3) *Rician-Faded R-Channel:* For the kth Rician-faded R-channel estimation error coefficient, we find that the average value of $\tilde{h}_{kI}$ is $\left[\sigma_n^2/(E_b+\sigma_n^2)\right]\sqrt{K/(1+K)}$ and the average of $\tilde{h}_{kQ}$ is zero, while both have equal variances. The total variance of $\tilde{h}_k$, i.e., $\sigma^2_{\tilde{h},\mathrm{Ri}}$, is twice the variance of $\tilde{h}_{kI}$ or $\tilde{h}_{kQ}$ and can thus be written as

$$\sigma^2_{\tilde{h},\mathrm{Ri}} = 2\left[\left(\frac{\sigma_n^2}{E_b+\sigma_n^2}\right)^2 \frac{1}{2(1+K)} + \frac{E_b\sigma_n^2}{2(E_b+\sigma_n^2)^2}\right] = \left(\frac{E_b}{\sigma_n^2}+1\right)^{-2}\left(\frac{E_b}{\sigma_n^2}+\frac{1}{1+K}\right) = (1+\bar{\gamma}_r)^{-2}\left(\bar{\gamma}_r+\frac{1}{1+K}\right). \tag{30}$$

Setting $K = 0$ in (30), we reobtain the expression for estimated error variance in Rayleigh channel (i.e., $\sigma^2_{\tilde{h},\mathrm{Ra}}$) given by (25).

In this work, we consider censoring of SUs based on the quality of the R-channel. The R-channel coefficient is estimated by the FC and if the estimated R-channel coefficient exceeds a censoring threshold (denoted as C_{th}), the corresponding SU is censored, i.e., it is allowed to transmit. Accordingly, the channel estimation is either perfect (with no estimation error) or imperfect (with an estimation error). *In the second transmission phase*, $\bar{K}$ selected SUs, out of N available SUs, send sequentially their binary local decisions to the FC, using BPSK, over the corresponding R-channels. The R-channels are assumed to be slowly faded so that the fading coefficient can be assumed as constant during the transmission of a decision symbol. The signal at the FC received from the kth selected SU is [20], [21]

$$y_{k,d} = m_k h_k + n_{k,d} \qquad k \in \left\{1, 2, \ldots, \bar{K}\right\} \tag{31}$$

where $n_{k,d} \sim \mathcal{CN}\left(0, \sigma_n^2\right)$ and $m_k \in \left\{+\sqrt{E_b}, -\sqrt{E_b}\right\}$ is a BPSK-modulated binary decision.

B. Censoring Rule for SUs Under Fading Channels

As per our censoring scheme, an SU (say the kth) is selected for transmission if the amplitude of its estimated R-channel fading coefficient $\hat{h}_k$ is above C_{th}. Therefore, the probability of selecting an SU is

$$\bar{p} = \Pr\left(|\hat{h}_k| > C_{\mathrm{th}}\right) = 1 - F(C_{\mathrm{th}}) \tag{32}$$

where $F(C_{\mathrm{th}})$ is the CDF of $|\hat{h}_k|$ evaluated at C_{th}. Approximate expressions for $F(C_{\mathrm{th}})$ will be provided below, depending on the type of fading. At this point, for a given value of the threshold C_{th}, one can evaluate the probability of selecting an SU. Since N is the total number of SUs, the probability of selecting $\bar{K}$ of them, with corresponding R-channel fading coefficients higher than C_{th}, can be expressed as follows [20], [21]:

$$P(\bar{K}) = \binom{N}{\bar{K}} \bar{p}^{\bar{K}} (1-\bar{p})^{N-\bar{K}} \tag{33}$$

where $\bar{p}$ is given by (32).

1) *Rayleigh Fading Channel:* Since the amplitude of the estimated R-channel fading coefficient is Rayleigh distributed with parameter σ, we assume that $|\hat{h}_k|$ has approximately the same statistical distribution, i.e.,

$$F(C_{\mathrm{th}}) \simeq 1 - \exp\left(\frac{-C_{\mathrm{th}}^2}{2\sigma^2}\right). \tag{34}$$

The probability of selecting an SU with Rayleigh-faded R-channel is obtained by substituting (34) in (32):

$$\bar{p}_{\mathrm{Ra}} = 1 - F(C_{\mathrm{th}}) = \exp\left(\frac{-C_{\mathrm{th}}^2}{2\sigma^2}\right). \tag{35}$$

2) *Hoyt (Nakagami-q) Fading Channel:* The PDF of the Hoyt fading coefficient is [26, (2)]

$$f_X(x) = \frac{x}{\sigma_1\sigma_2}\exp\left(-\frac{x^2}{4}\left[\frac{1}{\sigma_1^2}+\frac{1}{\sigma_2^2}\right]\right) \times I_0\left[\frac{x^2}{4}\left(\frac{1}{\sigma_2^2}-\frac{1}{\sigma_1^2}\right)\right]; \quad x \geq 0 \tag{36}$$

where $\sigma_1 = \sqrt{\Omega q^2/1+q^2}$; and $\sigma_2 = \sqrt{\Omega/1+q^2}$. Using (36) and [26, (58)], the CDF of the amplitude of the

estimated Hoyt fading coefficient can be approximated as

$$F(C_{\text{th}}) \simeq \frac{1}{2\sigma_1\sigma_2\sqrt{\mathcal{A}^2-\mathcal{B}^2}}\left[1+\exp\left(-\mathcal{A}C_{\text{th}}^2\right)\right. \\ \left.\times\, I_0\left(\mathcal{B}C_{\text{th}}^2\right) - Q(\mathcal{U}_3,\mathcal{V}_3)\right]; \quad C_{\text{th}} \geq 0 \tag{37}$$

where $\mathcal{U}_3 = \sqrt{(\mathcal{A}-\sqrt{\mathcal{A}^2-\mathcal{B}^2})C_{\text{th}}^2}$ and $\mathcal{V}_3 = \sqrt{(\mathcal{A}+\sqrt{\mathcal{A}^2-\mathcal{B}^2})C_{\text{th}}^2}$. The probability of selecting an SU is obtained by substituting (37) in (32), thus obtaining

$$\bar{p}_{\text{Ho}} \simeq 1 - \frac{1}{2\sigma_1\sigma_2\sqrt{\mathcal{A}^2-\mathcal{B}^2}}\left[1+\exp\left(-\mathcal{A}C_{\text{th}}^2\right)\right. \\ \left.\times I_0\left(\mathcal{B}C_{\text{th}}^2\right) - Q(\mathcal{U}_3,\mathcal{V}_3)\right]. \tag{38}$$

3) *Rician Fading Channel:* In the case of Rician-faded R-channel, the amplitude of the estimated R-channel fading coefficient is approximated as a Rician-distributed random variable, so that its CDF can be written as

$$F(C_{\text{th}}) \simeq 1 - Q\left(\frac{S}{\sigma}, \frac{C_{\text{th}}}{\sigma}\right); \quad C_{\text{th}} \geq 0 \tag{39}$$

where $S = \sqrt{K\Omega/(1+K)}$ and $\sigma = \sqrt{\Omega/2(1+K)}$. The probability of selecting an SU is directly obtained by substituting (39) in (32):

$$\bar{p}_{\text{Ri}} \simeq Q\left(\frac{S}{\sigma}, \frac{C_{\text{th}}}{\sigma}\right). \tag{40}$$

Denoting $P(\text{md}|\bar{K})$ and $P(\text{fa}|\bar{K})$ as the conditional miss detection and false alarm probabilities when decisions from $\bar{K}$ selected SUs are fused at the FC, the average probabilities of miss detection and false alarm can be expressed as follows:

$$\bar{Q}_m = P(\text{miss detection}) = \sum_{\bar{K}=0}^{N} P(\text{md}|\bar{K})P(\bar{K}), \tag{41}$$

$$\bar{Q}_f = P(\text{false alarm}) = \sum_{\bar{K}=0}^{N} P(\text{fa}|\bar{K})P(\bar{K}). \tag{42}$$

Therefore, the error rate with censoring can be expressed as follows:

$$\bar{Q} = P(\mathcal{H}_1)\bar{Q}_m + P(\mathcal{H}_0)\bar{Q}_f \tag{43}$$

where $\bar{Q}_m$ and $\bar{Q}_f$ are functions of C_{th}, $P(\text{md}|\bar{K})$, and $P(\text{fa}|\bar{K})$, which depend on the IED parameter, the SNRs of the S- and R-channels, and the local detection threshold λ at an SU. However, it may be observed that the error rate with censoring, as formulated in (43), incorporates the average miss detection and average false alarm probabilities, where the averaging is done over the distribution of the censored SUs over a single hop transmission from SUs to FC. In contrast, the error rate as defined in [34] considers false alarm and miss detection at the FC using multi hop transmission by SUs with no censoring of SUs.

C. Fusion Rules

The FC, upon reception of local decisions from selected SUs, makes a decision on the phenomenon status, i.e., $\mathcal{H}_1$ or $\mathcal{H}_0$ according to a fusion rule. Due to the noise and fading in the R-channel, the associated decision might differ from the one sent by the corresponding SU.

1) *Majority-Logic Fusion Rule:* The decision received from the kth selected SU is

$$d_k = \begin{cases} 1 & \text{if the decision is in favor of } \mathcal{H}_1 \\ 0 & \text{if the decision is in favor of } \mathcal{H}_0 \end{cases} \tag{44}$$

where $k \in \{1, 2, \ldots, \bar{K}\}$. The decisions from all the SUs are, first, decoded. In principle, there can be decoding errors. However, in this work, we assume error-free decoding, and then, the FC makes a global decision d_0 according to the following general majority-logic-like rule [37]:

$$d_0 = \begin{cases} \mathcal{H}_1 & \text{if} \quad \sum_{k=1}^{\bar{K}} d_k > \left\lfloor \bar{K}/2 \right\rfloor \\ \mathcal{H}_0 & \text{if} \quad \sum_{k=1}^{\bar{K}} d_k \leq \left\lfloor \bar{K}/2 \right\rfloor. \end{cases} \tag{45}$$

Sometimes, if the number of decisions in favor of $\mathcal{H}_1$ is equal to the number of decisions in favor of $\mathcal{H}_0$, then the FC flips a fair coin and takes a decision in favor of either $\mathcal{H}_1$ or $\mathcal{H}_0$. It may be observed that, in the case without censoring, the value of $\bar{K}$ in above expression (45) needs to be replaced by total number N of available SUs.

2) *MRC Fusion Rule:* The MRC fusion rule depends on the channel estimates and on the SU's performance metrics (probabilities of correct detection $P_d = 1 - P_m$ and of false alarm P_f), incorporating the effect of the channel estimation error. Assuming that the selected SUs have identical values of P_d and P_f and BPSK is the used modulation format, the MRC fusion rule can be obtained from an approximated likelihood ratio test (LRT) fusion rule for low R-channel SNR [31], [38]:

$$\Lambda_{\text{lrt}} = \frac{2\sqrt{E_b}}{\sigma_w^2}\sum_{k=1}^{\bar{K}}(P_{d,k} - P_{f,k})\text{Re}(y_{k,d}\hat{h}_k^*). \tag{46}$$

Under the assumption that the selected SUs have identical local performance metrics, (46) can be simplified further as

$$\Lambda_{\text{mrc}} = \sum_{k=1}^{\bar{K}} \text{Re}(y_{k,d}\hat{h}_k^*) \tag{47}$$

where $\hat{h}_k^*$ is the complex conjugate of the estimated channel coefficient $\hat{h}_k$. Given $\hat{h}_k$, one can observe from (47) that Λ_{mrc} is a linear combination of Gaussian random variables and, therefore, has a Gaussian distribution. Next, the FC can take a decision in favor of $\mathcal{H}_1$ or $\mathcal{H}_0$ by simply comparing Λ_{mrc} with a threshold set to zero. Equation (47) can be simplified further, to analyze the performance of an equal gain combiner (EGC), as follows:

$$\Lambda_{\text{egc}} = \sum_{k=1}^{\bar{K}} \text{Re}\left(y_{k,d}\frac{\hat{h}_k^*}{|h_k|}\right). \tag{48}$$

This work could be extended to considering LLR-based fusion rule.

3) *Optimum Values of C_{th} for CED and IED:* There exists an optimal value of C_{th} for which $\bar{Q}_m$ is minimized. In this section, we evaluate analytically this optimum value

in the presence of a Rayleigh-faded R-channel. We first derive an analytical closed-form expression for $\bar{Q}_m$, assuming majority-logic fusion at FC, under Rayleigh fading. Next, the optimal value of C_{th} is evaluated for both CED and IED cases. In (41), $P(\text{md}|\bar{K})$ under majority-logic fusion can be expressed as

$$P(\text{md}|\bar{K}) = 1 - \sum_{i=\lfloor \bar{K}/2+1 \rfloor}^{\bar{K}} \binom{\bar{K}}{i} P_d^i (1-P_d)^{\bar{K}-i} \quad (49)$$

where P_d is the probability of detection in individual CR at the FC after sending the decision over a faded R-channel. Expression (41) can be rewritten, by using (33) and (49), as

$$\begin{aligned}\bar{Q}_m &= \sum_{\bar{K}=0}^{N} \left\{ 1 - \sum_{i=\lfloor \bar{K}/2+1 \rfloor}^{\bar{K}} \binom{\bar{K}}{i} P_d^i (1-P_d)^{\bar{K}-i} \right\} \\ &\quad \times \binom{N}{\bar{K}} \bar{p}^{\bar{K}} (1-\bar{p})^{N-\bar{K}} \\ &= 1 - \sum_{\bar{K}=0}^{N} \sum_{i=\lfloor \bar{K}/2+1 \rfloor}^{\bar{K}} \binom{\bar{K}}{i} P_d^i (1-P_d)^{\bar{K}-i} \\ &\quad \times \binom{N}{\bar{K}} \bar{p}^{\bar{K}} (1-\bar{p})^{N-\bar{K}}. \end{aligned} \quad (50)$$

The probability $\bar{Q}_m$ can thus be minimized to derive an optimal value of C_{th}, by setting the partial derivative of (50), with respect to C_{th}, to zero, i.e., $\partial \bar{Q}_m / \partial C_{\text{th}} = 0$. Initially, we assume that

$$\frac{\partial \bar{Q}_m}{\partial C_{\text{th}}} = \frac{\partial \bar{Q}_m}{\partial \bar{p}} \times \frac{\partial \bar{p}}{\partial C_{\text{th}}}. \quad (51)$$

The solution of the first part in (51) can be obtained by partially differentiating (50) with respect to $\bar{p}$, obtaining

$$\begin{aligned}\frac{\partial \bar{Q}_m}{\partial \bar{p}} &= 1 - \sum_{\bar{K}=0}^{N} \sum_{i=\lfloor \bar{K}/2+1 \rfloor}^{\bar{K}} \binom{\bar{K}}{i} P_d^i (1-P_d)^{\bar{K}-i} \binom{N}{\bar{K}} \\ &\quad \times \left\{ \bar{p}^{\bar{K}-1} (1-\bar{p})^{N-\bar{K}} \left[\bar{K}(1-\bar{p}) - \bar{p}(N-\bar{K}) \right] \right\}. \end{aligned} \quad (52)$$

Since from (35), $\bar{p}_{\text{Ra}} = \exp(-C_{\text{th}}^2/2\sigma^2)$ for a Rayleigh fading channel, the second part in (51) can be obtained by partially differentiating (35) with respect to C_{th}

$$\frac{\partial \bar{p}}{\partial C_{\text{th}}} = -\frac{C_{\text{th}}}{\sigma^2} \exp\left(-\frac{C_{\text{th}}^2}{2\sigma^2} \right). \quad (53)$$

By substituting (52) and (53) into (51), we obtain

$$\begin{aligned}\frac{\partial \bar{Q}_m}{\partial C_{\text{th}}} &= -\sum_{\bar{K}=0}^{N} \sum_{i=\lfloor \bar{K}/2+1 \rfloor}^{\bar{K}} \binom{\bar{K}}{i} P_d^i (1-P_d)^{\bar{K}-i} \binom{N}{\bar{K}} \\ &\quad \times \left\{ \bar{p}^{\bar{K}-1} (1-\bar{p})^{N-\bar{K}} \left[\bar{K}(1-\bar{p}) - \bar{p}(N-\bar{K}) \right] \right\} \\ &\quad \times \left[-\frac{C_{\text{th}}}{\sigma^2} \exp\left(-\frac{C_{\text{th}}^2}{2\sigma^2} \right) \right]. \end{aligned} \quad (54)$$

TABLE III
Optimal Values of C_{th} for CED ($p = 2$) and IED ($p = 4$)

Detector type	λ_n	P_d at FC	Optimal C_{th} by analytically	Optimal C_{th} by simlation
IED	30	0.7041	0.4535	0.4500
CED	30	0.6574	0.4295	0.4295
IED	60	0.6986	0.4500	0.4450
CED	60	0.5599	0.4100	0.4100

Note that in the case with $\bar{K} = 0$, $P(0) = (1-\bar{p})^N$, then $\bar{Q}_m$ becomes

$$\begin{aligned}\bar{Q}_m &= \sum_{\bar{K}=1}^{N} \left(Q_m|\bar{K} \right) P(\bar{K}) + (Q_m|0)\bar{p}(0) \\ &= \sum_{\bar{K}=1}^{N} \left(Q_m|\bar{K} \right) P(\bar{K}) + 0.5(1-\bar{p})^N. \end{aligned} \quad (55)$$

It is assumed that when $\bar{K} = 0$, the FC flips a fair coin to decide about PU, so that $Q_m|0 = 0.5$. Finally, in the case with $\bar{K} = 0$, $\partial \bar{Q}_m / \partial C_{\text{th}}$ becomes

$$\begin{aligned}\frac{\partial \bar{Q}_m}{\partial C_{\text{th}}} &= \left\{ \sum_{\bar{K}=0}^{N} \sum_{i=\lfloor \bar{K}/2+1 \rfloor}^{\bar{K}} \binom{\bar{K}}{i} P_d^i (1-P_d)^{\bar{K}-i} \binom{N}{\bar{K}} \right. \\ &\quad \times \bar{p}^{\bar{K}-1} (1-\bar{p})^{N-\bar{K}-1} (\bar{K} - N\bar{p}) \\ &\quad \left. + 0.5N(1-\bar{p})^{N-1} \right\} \\ &\quad \times \left[\frac{C_{\text{th}}}{\sigma^2} \exp\left(-\frac{C_{\text{th}}^2}{2\sigma^2} \right) \right] = 0. \end{aligned} \quad (56)$$

Since the second term [.] in (56) is not equal to zero, the first term {.} in (56) is equal to zero, i.e.,

$$\begin{aligned}\frac{\partial \bar{Q}_m}{\partial C_{\text{th}}} &= \left\{ \sum_{\bar{K}=0}^{N} \sum_{i=\lfloor \bar{K}/2+1 \rfloor}^{\bar{K}} \binom{\bar{K}}{i} P_d^i (1-P_d)^{\bar{K}-i} \binom{N}{\bar{K}} \right. \\ &\quad \left. \times \bar{p}^{\bar{K}-1} (1-\bar{p})^{N-\bar{K}-1} (\bar{K} - N\bar{p}) + 0.5N(1-\bar{p})^{N-1} \right\} = 0. \end{aligned} \quad (57)$$

By solving (57) numerically, we get optimal value of $\bar{p}$. From the optimal value of $\bar{p}$, one can obtain an optimal value of C_{th}, denoted as $C_{\text{th-opt}}$. The optimal values of C_{th} for both IED and CED under Rayleigh fading case are listed in Table III. The same approach can be followed to derive the closed-form expressions for $\bar{Q}_f$ (and its corresponding $\partial \bar{Q}_f / \partial C_{\text{th}}$) and $\bar{Q}$ (and its corresponding $\partial \bar{Q} / \partial C_{\text{th}}$). Then, an optimal C_{th} can be evaluated by setting $\partial \bar{Q}_f / \partial C_{\text{th}}$ or $\partial \bar{Q} / \partial C_{\text{th}}$ to zero. Table III shows optimal values of C_{th} for both IED and CED for two different values of λ_n. It can be observed that the optimal values of C_{th} obtained analytically matches almost perfectly with the simulated values. The CSS system parameters are set to $\bar{\gamma}_s = 20$ dB, $\bar{\gamma}_r = -7$ dB, $N = 30$, and $M = 2$.

TABLE IV
Network Parameters Used for Simulation

Description	Notation	Values
Number of available SUs	N	10, 30
IED parameter	p	2 or 4
Number of antennas at each IED	M	1, 2, 5
Average S-channel SNR	$\bar{\gamma}_s$	15 dB, 20 dB
Average R-channel SNR	$\bar{\gamma}_r$	−7 dB, −9 dB
Censoring threshold	C_{th}	0 to 3
Normalized detection threshold at SU	λ_n	30, 60
Rician fading parameter	K	0, 2, 3
Hoyt fading parameter	q	0.5, 1

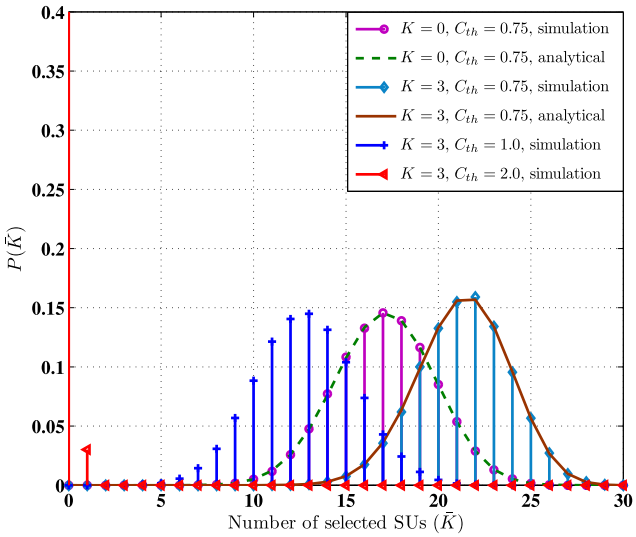

Fig. 9. PMF of the number of selected SUs for different values of C_{th} under perfect channel estimation in Rician (K set to 0 or 3) faded channel, with $N = 30$.

V. PERFORMANCE ANALYSIS OF CSS: NOISY AND FADED REPORTING CHANNELS

As in Section III, the following results are also obtained using simulations. The performance of CSS system has been evaluated for both perfect and imperfect channel estimation in Rayleigh-, Rician-, and Hoyt-faded environments for various configurations of the main network parameters, such as C_{th}, N, M, λ_n, $\bar{\gamma}_s$, and $\bar{\gamma}_r$. The average miss detection probability ($\bar{Q}_m$) and the error rate ($\bar{Q}$) are also evaluated through simulations. In the following figures, the performance curves with CED are associated with $p = 2$, while those relative to IED are associated with $p = 4$. Table IV shows the values of the relevant network parameters used in the simulation study.

In Fig. 9, the impact of Rician fading parameter K on the binomially distributed PMF of the number of selected SUs is shown. It can be observed that the number of selected SUs increases for reducing fading severity in the R-channel, i.e., when increasing the value of the parameter K from 0 to 3. We remark that, for $K = 0$, the PMF in the Rayleigh-faded case is obtained [20]. The simulation-based binomially distributed PMF of the number of selected SUs

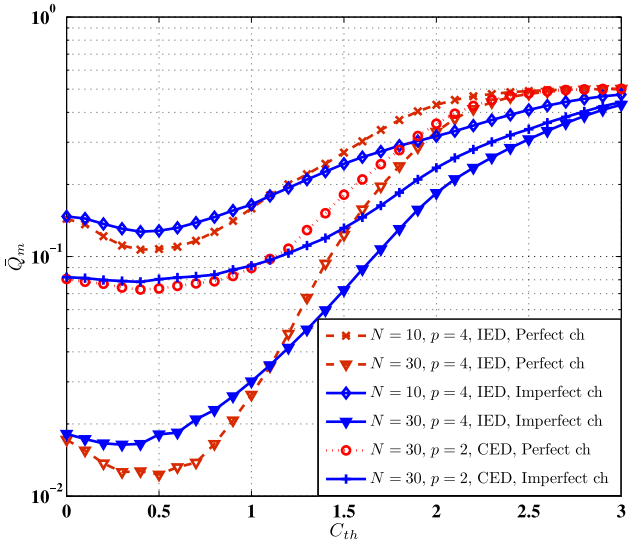

Fig. 10. $\bar{Q}_m$, as a function of C_{th} for various values of N in Rayleigh fading, (majority-logic fusion, $\bar{\gamma}_s = 20$ dB, $\bar{\gamma}_r = -7$ dB, $\lambda_n = 30$, and $M = 2$, and $P_f = 8 \times 10^{-3}$).

matches exactly with the analytical expression given in (40) and (33). This validates our analytical framework.

In Fig. 10, the impact of C_{th} on $\bar{Q}_m$ is investigated, under both perfect and imperfect channel estimation. From the obtained results, it can be observed that as C_{th} increases, $\bar{Q}_m$ attains a minimum value in correspondence to an "optimal" value of C_{th} and, thereafter, increases (up to 0.5) for increasing values of C_{th}. The optimal value of C_{th} depends on the channel estimation strategy. For example, for $p = 4$ and $N = 30$, optimal values of C_{th} are found to be approximately equal to 0.5 for perfect channel estimation and to 0.3 for imperfect channel estimation. This behavior of $\bar{Q}_m$ is due to the different PMF of the number of censored SUs for different values of C_{th} (as shown in Fig. 9). For very small values of C_{th}, even unreliable links tend to be selected and $\bar{Q}_m$ is rather high. On the other hand, as C_{th} becomes very high, no SU is selected to transmit, i.e., $P(0) = 1$, and the FC takes a decision by flipping a fair coin, thus setting $\bar{Q}_m = 0.5$. Furthermore, as expected, a large number of SUs leads to a reduced value of $\bar{Q}_m$. More precisely, $\bar{Q}_m$ reduces significantly, with respect to CED, for both the cases of perfect and imperfect channel estimation. In particular, for $C_{\text{th}} = 0.5$ and $N = 30$, $\bar{Q}_m$ decreases by 83.3% in the presence of perfect channel estimation and by 77.5% in the presence of imperfect channel estimation, as p increases from 2 to 4.

In Fig. 11, the impact of C_{th} on the error rate in the presence of censoring, under perfect channel estimation, is investigated. It can be seen, from the obtained results, that as C_{th} increases, $\bar{Q}$ attains a minimum value in correspondence to an "optimal" value of C_{th} and, thereafter, increases for further increasing values of C_{th} to finally attain a value equal to 1 ($\bar{Q}_m$, as well as $\bar{Q}_f$, reaches a value equal to 0.5). The obtained results show the existence of an optimal value of the C_{th}, in correspondence to which $\bar{Q}$ is minimized. The optimum value of C_{th} depends on the channel estimation

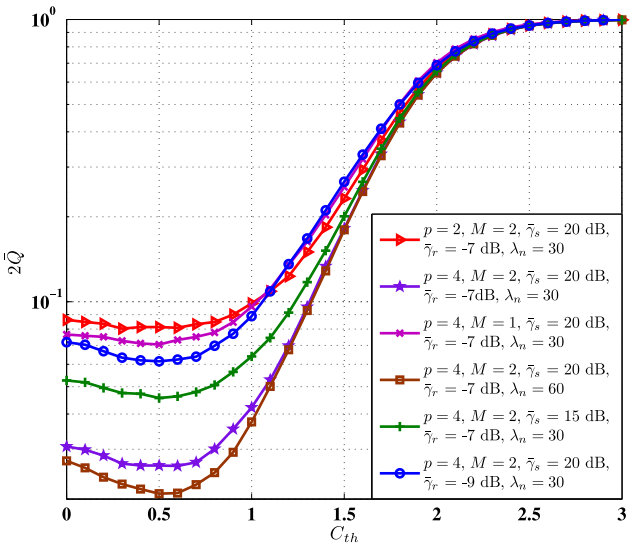

Fig. 11. $2\bar{Q}$, as a function of C_{th}, for various values of p, M, λ_n, $\bar{\gamma}_s$ and $\bar{\gamma}_r$ in Rayleigh fading (majority-logic fusion).

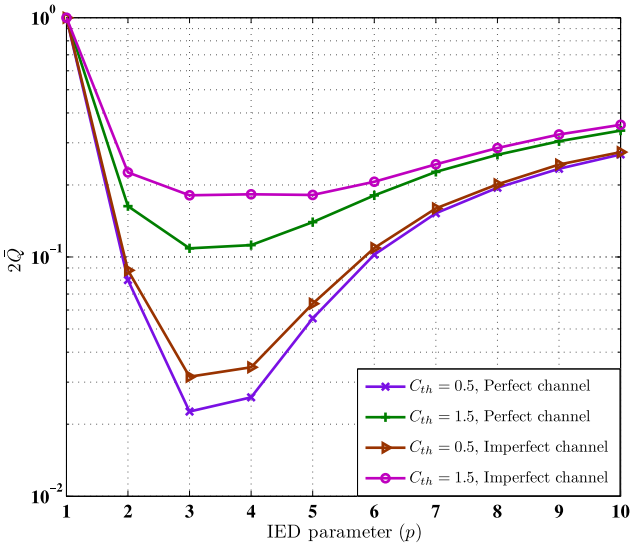

Fig. 12. $2\bar{Q}$, as a function of p, for different values of C_{th} (majority-logic fusion, Rayleigh fading, $N = 30$, $M = 2$, $\lambda_n = 30$, $\bar{\gamma}_s = 20$ dB, and $\bar{\gamma}_s = -7$ dB).

strategy; the values of $\bar{\gamma}_s$ as well as $\bar{\gamma}_r$; the values of p, M, and λ_n. The optimum value of C_{th} is 0.5 ($\bar{Q}$ is 1.2×10^{-2}) for $p = 4$, $M = 2$, $\lambda_n = 30$, $\bar{\gamma}_s = 20$ dB, and $\bar{\gamma}_r = -7$ dB.

In Fig. 12, the error rate with censoring is shown, as a function of p, under perfect and imperfect channel estimation. It can be observed that there exists an "optimal" value of p, which minimizes the error rate. From Figs. 11 and 12, it can be concluded that the optimum values of p and C_{th} are 3 and 0.5, respectively, considering IED-based CSS with threshold-based censoring.

In Fig. 13, the performances, in terms of average miss detection probabilities as functions of C_{th} with majority-logic and MRC fusions, are directly compared, for both the cases of perfect and imperfect channel estimation, in the presence of Rayleigh fading. When M increases, $\bar{Q}_m$

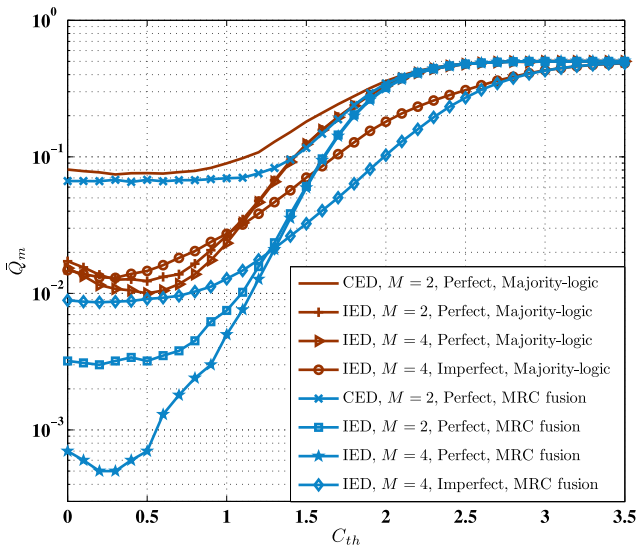

Fig. 13. Performance comparison, between majority-logic and MRC fusions, as function of C_{th}, in Rayleigh fading for different values of M ($N = 30$, $\bar{\gamma}_s = 20$ dB, $\bar{\gamma}_r = -7$ dB, $\lambda_n = 30$, and $P_f = 8 \times 10^{-3}$).

reduces with both types of fusions and channel estimation strategies. We observe that the performance with MRC fusion is better than the performance with majority-logic fusion with both channel estimation strategies. For example, in the case of perfect channel estimation, for $C_{\text{th}} = 0.3$ and $M = 4$, $\bar{Q}_m$ is 96% lower with MRC than with majority-logic fusion. Similarly, in the case of imperfect channel estimation, $\bar{Q}_m$ with MRC is 46.7% lower than that with majority-logic fusion for the same values of C_{th} and M. It can also be observed that $\bar{Q}_m$ reduces significantly with IED with respect to the case with CED. It can also be observed that an optimal censoring threshold depends on the value of M. For example, in the case of perfect channel estimation, MRC fusion, and $p = 4$ (i.e., IED with $p = 4$), the optimum value of C_{th} is found to be 0.2 and 0.25 for $M = 2$ and $M = 4$, respectively.

In Figs. 14 and 15, the impacts of the Hoyt parameter q and the Rician parameter K are investigated, respectively. The performance, with both majority-logic and MRC fusions, is evaluated for both perfect and imperfect channel estimations. The performance with $q = 1$ and $K = 0$ reduces to that of Rayleigh fading (as in Fig. 13). When q increases from 0.5 to 1 (in Fig. 14) and K increases from 0 to 2 (in Fig. 15) the fading severity in the both S- and R-channels decreases, so that the FC receives a larger number of correct decisions and this, in turns, leads to a reduction of $\bar{Q}_m$ and $\bar{Q}$. As in Fig. 13, in these cases, the error rate with MRC fusion is better than the performance with majority-logic fusion for both the cases of perfect and imperfect channel estimations. It can also be observed that $\bar{Q}_m$ and $\bar{Q}$ are significantly reduced with IED with respect to the case with CED.

In Fig. 16, the performance, without censoring and with censoring, is evaluated. It can be observed that the performance with censoring is better than the performance without censoring, as the error rate reduces significantly. In

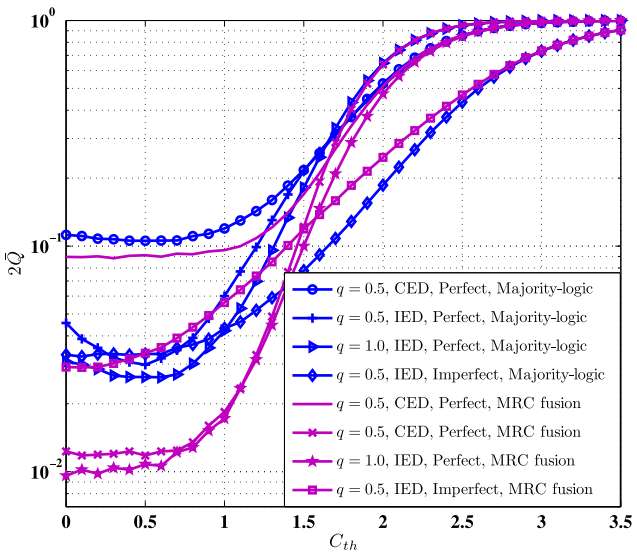

Fig. 14. Performance comparison, between majority-logic and MRC fusions, as functions of C_{th}, in Hoyt fading ($N = 30$, $\bar{\gamma}_s = 20$ dB, $\bar{\gamma}_r = -7$ dB, $\lambda_n = 30$, and $P_f = 8 \times 10^{-3}$).

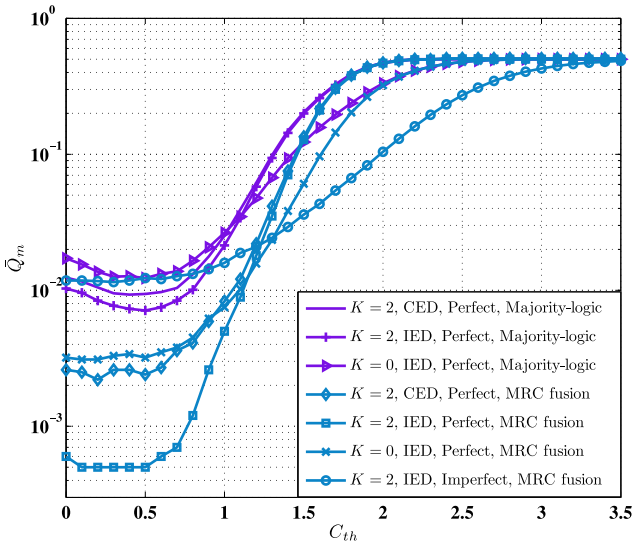

Fig. 15. Performance comparison, between majority-logic and MRC fusions, as function of C_{th}, in Rician fading ($N = 30$, $\bar{\gamma}_s = 20$ dB, $\bar{\gamma}_r = -7$ dB, $\lambda_n = 30$, and $P_f = 8 \times 10^{-3}$).

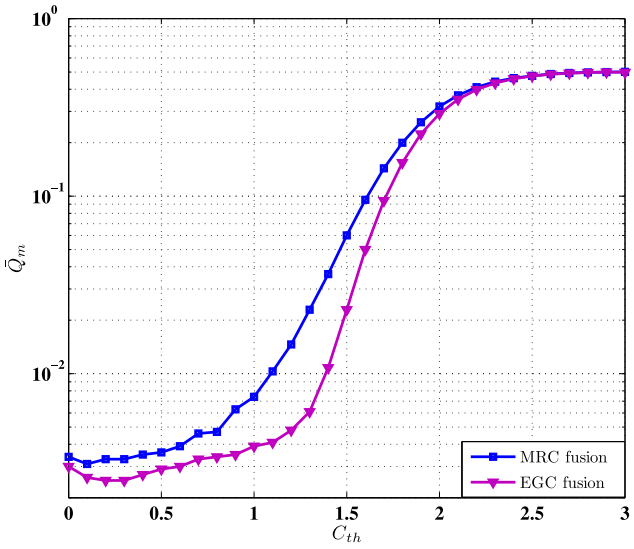

Fig. 16. Performance comparison, between CSS without censoring ($2Q$) and CSS with censoring ($2\bar{Q}$, perfect channel estimation, $C_{\text{th}} = 0.5$), as function of p, in Rayleigh fading (majority-logic fusion, $N = 10$, $M = 2$, $\bar{\gamma}_s = 20$ dB, $\bar{\gamma}_r = -7$ dB, and $\lambda_n = 30$).

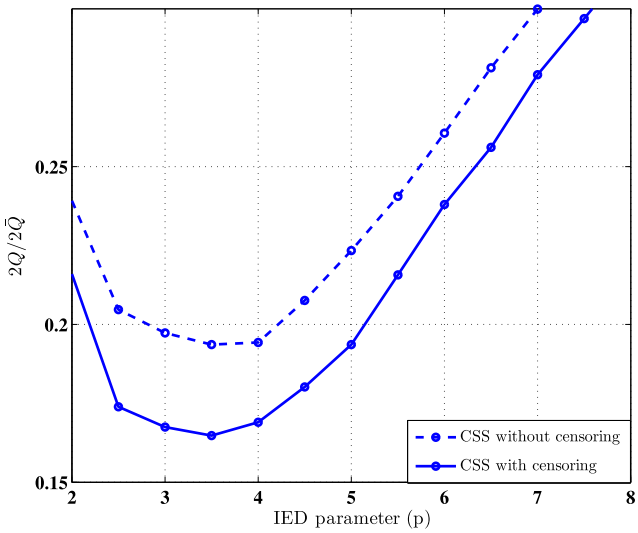

Fig. 17. Performance of MRC and EGC fusions, perfect channel estimation in Rayleigh fading ($N = 30$, $M = 2$, $\bar{\gamma}_s = 20$ dB, $\bar{\gamma}_r = -7$ dB, and $\lambda_n = 30$).

the case with censoring, even if a smaller number of SUs transmit their local decisions, a significant performance improvement is obtained with respect to the case without censoring, where all SUs transmit their local decisions but some of the decisions may be transmitted over less reliable (because of fading) R-channels. This means that censoring reduces the computations complexity, as the terminals from SUs associated with deeply faded R-channels is stopped and overall performance improves.

A comparative performance of MRC and EGC is shown in Fig. 17. EGC is seen to yield lower $\bar{Q}_m$ with respect to MRC, as observed in [30] and [31], where EGC leads to higher values of Q_d with respect to the case with MRC.

VI. CONCLUSION

We have investigated the performance of IED-based CSS with SUs censored on the basis of the quality of the R-channels in the presence of Rayleigh, Hoyt, and Rician fading environments. The censoring threshold for the selection of SUs has a significant impact on the average miss detection probability. The performance, with both perfect and imperfect channel estimation, has been evaluated and the two cases have been directly compared. Depending on the values of relevant network parameters (such as the IED parameter, the normalized detection threshold, the number of antennas, the average S-channel and R-channel SNRs), an optimum censoring threshold can be identified in correspondence to minimum values of the miss detection

probability and of the error rate. The average miss detection probability, as well as the error rate, reduces for increasing values of

1) the number of available SUs;
2) the number of antennas;
3) the average S-channel and R-channel SNRs, with both perfect and imperfect channel estimation.

The obtained results are expedient, for instance, to the design of CSS systems to prolong the lifetime of an energy-constrained CR networks.

REFERENCES

[1] S. Ball, A. Ferguson, and T. W. Rondeau
Consumer applications of cognitive radio defined networks
In *Proc. IEEE Int. Symp. New Frontiers Dyn. Spectr. Access Netw.*, Baltimore, MD, USA, Nov. 2005, pp. 518–525.

[2] A. Gorcin and H. Arslan
Public safety and emergency case communications: Opportunities from the aspect of cognitive radio
In *Proc. IEEE Symp. New Frontiers Dyn. Spectr. Access Netw.*, Chicago, IL, USA, Oct. 2008, pp. 1–10.

[3] M. Hoyhtya
Secondary terrestrial use of broadcasting satellite services below 3 Ghz
Int. J. Wireless Mobile Netw., vol. 5, no. 1, pp. 1–14, Feb. 2013.

[4] H. Urkowitz
Energy detection of unknown deterministic signals
Proc. IEEE, vol. 55, no. 4, pp. 523–231, Apr. 1967.

[5] Y. C. Liang, Y. Zeng, E. C. Y. Peh, and A. T. Hoang
Sensing-throughput tradeoff for cognitive radio networks
IEEE Trans. Wireless Commun., vol. 7, no. 4, pp. 1326–1337, Apr. 2008.

[6] E. C. Y. Peh, Y. C. Liang, Y. L. Guan, and Y. Zeng
Optimization of cooperative sensing in cognitive radio networks: A sensing-throughput tradeoff view
IEEE Trans. Veh. Technol., vol. 58, no. 9, pp. 5294–5299, Nov. 2009.

[7] F. F. Digham, M.-S. Alouini, and M. K. Simon
On the energy detection of unknown signals over fading channels
In *Proc. IEEE Inet. Conf. Commun.*, May 2003, pp. 3575–3579.

[8] W. Zhang, R. Mallik, and K. B. Letaief
Optimization of cooperative spectrum sensing with energy detection in cognitive radio networks
IEEE Trans. Wireless Commun., vol. 8, no. 12, pp. 5761–5766, Dec. 2009.

[9] A. Singh, M. R. Bhatnagar, and R. K. Mallik
Cooperative spectrum sensing in multiple antenna based cognitive radio network using an improved energy detector
IEEE Commun. Lett., vol. 16, no. 1, pp. 64–67, Jan. 2012.

[10] A. Singh, M. R. Bhatnagar, and R. K. Mallik
Cooperative spectrum sensing with an improved energy detector in cognitive radio network
In *Proc. IEEE Nat. Conf. Commun.*, Bangalore, India, Jan. 2011, pp. 1–5.

[11] A. Singh, M. R. Bhatnagar, and R. K. Mallik
Optimization of cooperative spectrum sensing with an improved energy detector over imperfect reporting channels
In *Proc. IEEE Veh. Technol. Conf.*, San Francisco, CA, USA, Sep. 2011, pp. 1–5.

[12] S. Nallagonda, A. Chandra, S. D. Roy, and S. Kundu
Detection performance of cooperative spectrum sensing over Hoyt and Rican faded sensing channels
IEICE Commun. Express, vol. 2, no. 7, pp. 319–324, Jul. 2013.

[13] S. Nallagonda, A. Chandra, S. D. Roy, and S. Kundu
On performance of cooperative spectrum sensing based on improved energy detector with multiple antennas in Hoyt fading channel
In *Proc. Annu. IEEE India Conf.*, Dec. 2013, pp. 1–6.

[14] K. Umebayashi, J. J. Lehtomaki, T. Yazawa, and Y. Suzuki
Efficient decision fusion for cooperative spectrum sensing based on OR rule
IEEE Trans. Wireless Commun., vol. 11, no. 7, pp. 2585–2595, Jul. 2012.

[15] J. Ma, G. Zhao, and Y. (G.) Li
Soft combination and detection for cooperative spectrum sensing in cognitive radio networks
IEEE Trans. Wireless Commun., vol. 7, no. 11, pp. 4502–4507, Nov. 2008.

[16] P. Salvo Rossi, D. Ciuonzo, and G. Romano
Orthogonality and cooperation in collaborative spectrum sensing through MIMO decision fusion
IEEE Trans. Wireless Commun., vol. 12, no. 11, pp. 5826–5836, Nov. 2013.

[17] C. Rago, P. Willett, and Y. Bar-Shalom
Censoring sensors: A low-communication-rate scheme for distributed detection
IEEE Trans. Aerosp. Electron. Syst., vol. 32, no. 2, pp. 554–568, Apr. 1996.

[18] I. Nevat, G. W. Peters, and I. B. Collings
Distributed detection in sensor networks over fading channels with multiple antennas at the fusion centre
IEEE Trans. Signal Process., vol. 62, no. 3, pp. 671–683, Feb. 2014.

[19] P. S. Rossi, D. Ciuonzo, K. Kansanen, and T. Ekman
On energy detection for MIMO decision fusion in wireless sensor networks over NLOS fading
IEEE Commun. Lett., vol. 19, no. 2, pp. 303–306, Feb. 2015.

[20] S. Nallagonda, S. D. Roy, S. Kundu, G. Ferrari, and R. Raheli
Cooperative spectrum sensing with censoring of cognitive radios in fading channel under majority logic fusion
In *Cognitive Communication and Cooperative HetNet Coexistence*, M. G. Di Benedetto and F. Bader, Eds. Basel, Switzerland: Springer Feb. 2014, ch. 7, pp. 133–162.

[21] S. Nallagonda, S. D. Roy, S. Kundu, G. Ferrari, and R. Raheli
Cooperative spectrum sensing with censoring of cognitive radios with majority logic fusion in Hoyt fading
In *Proc. IEEE Int. Conf. Adv. Netw. Telecommun. Syst.*, Chennai, India, Dec. 2013, pp. 1–6.

[22] S. Nallagonda, S. D. Roy, and S. Kundu
Cooperative spectrum sensing with censoring of improved energy detector based cognitive radios in Rayleigh faded channel
Int. J. Wireless Inf. Netw., vol. 21, no. 1, pp. 74–88, Mar. 2014.

[23] C. Sun, W. Zhang, and K. B. Leataief
Cooperative spectrum sensing for cognitive radios under bandwidth constraints
In *Proc. IEEE Wireless Commun. Netw. Conf.*, Mar. 2007, pp. 1–5.

[24] M. K. Simon and M. S. Alouini
Digital Communication Over Fading Channels, 2nd ed. Hoboken, NJ, USA: Wiley, Dec. 2004.

[25] A. Chandra, C. Bose, and M. K. Bose
Performance of non-coherent MFSK with selection and switched diversity over Hoyt fading channel
Wireless Pers. Commun., vol. 68, no. 2, pp. 379–399, Jan. 2013.

[26] A. Chandra, C. Bose, and M. K. Bose
Symbol error probability of non-coherent M-ary frequency shift keying with postdetection selection and switched combining over Hoyt fading channel
IET Commun., vol. 6, no. 12, pp. 1692–1701, Aug. 2012.

[27] D. Ciuonzo, A. De Maio, and P. S. Rossi
A systematic framework for composite hypothesis testing of independent Bernoulli trials
IEEE Signal Process. Lett., vol. 22, no. 9, pp. 1249–1253, Sep. 2015.

[28] M. Fernandez and S. Williams
Closed-form expression for the poisson-binomial probability density function
IEEE Trans. Aerosp. Electron. Syst., vol. 46, no. 2, pp. 803–817, Apr. 2010.

[29] B. Chen, R. Jiang, T. Kasetkasem, and P. K. Varshney
Channel aware decision fusion in wireless sensor networks
IEEE Trans. Signal Process., vol. 52, no. 12, pp. 3454–3458, Dec. 2004.

[30] Y. Lin, B. Chen, and P. K. Varshney
Decision fusion rules in multi-hop wireless sensor networks
IEEE Trans. Aerosp. Electron. Syst., vol. 41, no. 2, pp. 475–488, Apr. 2005.

[31] R. Niu, B. Chen, and P. K. Varshney
Fusion of decisions transmitted over Rayleigh fading channels in wireless sensor networks
IEEE Trans. Signal Process., vol. 54, no. 3, pp. 1018–1027, Mar. 2006.

[32] P. Jacob, S. Rajendra Prasad, A. S. Madhukumar, and V. A. Prasad
Cognitive radio for aeronautical communications: A survey
IEEE Access, vol. 4, pp. 3417–3443, May 2016.

[33] J. I. Marcum
A statistical theory of target detection by pulsed radar
Rand Corporation, Santa Monica, CA, USA, Air Force Project RAND Research Memorandum RM-754, Dec. 1947, pp. 159–160.

[34] A. Singh, M. R. Bhatnagar, and R. K. Mallik
Performance of an improved energy detector in multihop cognitive radio networks
IEEE Trans. Veh. Technol., vol. 65, no. 2, pp. 732–743, Feb. 2016.

[35] H. L. Van Trees
Detection, Estimation, and Modulation Theory-Part 1. New York, NY, USA: Wiley, 1968.

[36] A. H. Nuttall
Some integrals involving the QM function
IEEE Trans. Inf. Theory, vol. 21, no. 1, pp. 95–96, Jan. 1975.

[37] G. Ferrari and R. Pagliari
Decentralized binary detection with noisy communication links
IEEE Trans. Aerosp. Electron. Syst., vol. 42, no. 4, pp. 1554–1563, Oct. 2006.

[38] H. R. Ahmadi and A. Vosoughi
Impact of channel estimation error on decentralized detection in bandwidth constrained wireless sensor networks
In *Proc. IEEE Mil. Commun. Conf.*, San Diego, CA, USA, Nov. 2008, pp. 1–7.

Srinivas Nallagonda (M'16) received the B.E. degree in electronics and communication engineering from Osmania University, Hyderabad, India, in 2006, the M.Tech. degree in telecommunication engineering, and the Ph.D. degree in wireless communications from NIT Durgapur, Durgapur, India, in 2009 and 2014, respectively.

He served as an Assistant Professor from 2009 to 2010 in Swami Ramananda Tirtha Institute of Science & Technology and from 2014 to 2016 in Maturi Venkata Subba Rao Engineering College. He is currently working as an Associate Professor in the Department of ECE, M.L.R Institute of Technology and Management, Dundigal, India, affiliated to JNTU Hyderabad, India. His research interests include fading models, diversity techniques, and spectrum sensing issues in cognitive radio networks. As of today, he has published more than 40 research papers in various international conferences, journals, and book chapters.

Dr. Nallagonda also served as a Reviewer for several IEEE conferences.

Sanjay Dhar Roy (M'08) received the B.E. (Hons.) degree in electronics and telecommunication engineering from Jadavpur University, Kolkata, India, in 1997, the M.Tech. degree in telecommunication engineering, and the Ph.D. degree in electronics and communication engineering from NIT Durgapur, Durgapur, India, in 2008 and 2011, respectively.

He worked for Koshika Telecom Ltd., from 1997 to 2000. In 2000, he joined the Department of Electronics and Communication Engineering, National Institute of Technology Durgapur, as a Lecturer, where he is currently an Assistant Professor. His research interests include radio resource management, handoff, D2D communication, next generation cellular systems, and cognitive radio networks. As of today, he has published hundred (100) research papers in various journals and conferences.

Dr. Roy is a member of IEEE (Communication Society) and is a Reviewer of *IET Communications*, *Electronics Letters* and *Journal of PIER*, IJCS, Wiley, *International Journal of Electronics,* Taylor & Francis. He is also a Reviewer for IEEE Globecom, IEEE VTC, and IEEE PIMRC.

Sumit Kundu (SM'07) received the B.E. (Hons.) degree in electronics and communication engineering from National Institute of Technology, Durgapur, India, in 1991, and the M.Tech. degree in telecommunication systems engineering and the Ph.D. degree in wireless communication engineering from IIT Kharagpur, Kharagpur, India, respectively.

Since 1995, he has been a faculty in the Department of ECE, NIT Durgapur, where he is currently a Full time Professor. His research interests include wireless ad hoc and sensor networks, cognitive radio networks, cooperative communication, energy harvesting, and physical layer security in wireless networks. As of today, he has published more than 150 research papers in various journals and conferences.

Dr. Kundu is a Reviewer of several IEEE and Elsevier journals.

Gianluigi Ferrari (SM'12) received *Laurea* degree (5-year program, *summa cum laude*) in electrical engineering and Ph.D. degree in information technologies from the University of Parma, Parma, Italy, in 1998 and 2002, respectively.

He is an Associate Professor of telecommunications with the University of Parma, Parma, Italy. Since 2006, he has been the Coordinator of the Internet of Things (IoT) Laboratory (http://IoTlab.unipr.it) in the Department of Engineering and Architecture. As of today, he has published more than 250 papers (journals and conferences) and book chapters, receiving a few technical awards. He coauthored seven books. His research interests include signal processing, advanced communication and networking, and IoT and smart systems (http://www.tlc.unipr.it/ferrari).

Riccardo Raheli (M'87) is a Professor of communication engineering with the University of Parma, Parma, Italy, where he has held various positions since 1991. From 1988 to 1991, he was with the Scuola Superiore S. Anna, Pisa, Italy. From 1986 to 1988, he was with Siemens Telecomunicazioni, Milan, Italy. In 1990 and 1993, he was a Visiting Assistant Professor with the University of Southern California, Los Angeles, CA, USA. His scientific interests include the general area of systems for communication, processing and storage of information, in which he has published extensively in quality journals, conference proceedings, scientific monographs, and industrial patents.

Dr. Raheli has served as Editorial Board Member and Technical Program Committee Cochair of prestigious international journals and conferences.